Published in final edited form as:
J Neurosci Methods. 2009 July 30; 181(2): 212–226. doi:10.1016/j.jneumeth.2009.05.006.

Transgenic mice expressing a cameleon fluorescent Ca^{2+} indicator in astrocytes and Schwann cells allow study of glial cell Ca^{2+} signals *in situ* and *in vivo*

Stan D. Atkin[1], **Sundip Patel**[1], **Ara Kocharyan**[2], **Lynne A. Holtzclaw**[1], **Susanna H. Weerth**[1], **Vincent Schram**[3], **James Pickel**[4], and **James T. Russell**[1]

[1]Section on Cell Biology and Signal Transduction, NICHD, NIH, Bethesda, MD

[2]Laboratory of Functional and Molecular Imaging, NINDS, Bethesda, MD

[3]NICHD Microscopy and Imaging Core, NIMH, Bethesda, MD

[4]NIMH Transgenic Core Facility, NIMH, Bethesda, MD

Abstract

Glial cell Ca^{2+} signals play a key role in glial-neuronal and glial-glial network communication. Numerous studies have thus far utilized cell-permeant and injected Ca^{2+} indicator dyes to investigate glial Ca^{2+} signals *in vitro* and *in situ*. Genetically encoded fluorescent Ca^{2+} indicators have emerged as novel probes for investigating cellular Ca^{2+} signals. We have expressed one such indicator protein, the YC 3.60 cameleon, under the control of the S100β promoter and directed its expression predominantly in astrocytes and Schwann cells. Expression of YC 3.60 extended into the entire cellular cytoplasmic compartment and the fine terminal processes of protoplasmic astrocytes and Schwann cell Cajal bands. In the brain, all the cells known to express S100β in the adult or during development, expressed YC 3.60. While expression was most extensive in astrocytes, other glial cell types that express S100β, such as NG2 and CNP-positive oligodendrocyte progenitor cells (OP cells), microglia, and some of the large motor neurons in the brain stem, also contained YC 3.60 fluorescence. Using a variety of known *in situ* and *in vivo* assays, we found that stimuli known to elicit Ca^{2+} signals in astrocytes caused substantial and rapid Ca^{2+} signals in the YC 3.60-expressing astrocytes. In addition, forepaw stimulation while imaging astrocytes through a cranial window in the somatosensory cortex in live mice, revealed robust evoked and spontaneous Ca^{2+} signals. These results, for the first time, show that genetically encoded reporter is capable of recording activity-dependent Ca^{2+} signals in the astrocyte processes, and networks.

Keywords

YC 3.60 cameleon; Astrocytes; Schwann cells; Transgenic mice

Address all correspondence to: Dr. James T. Russell, Laboratory of Cellular and Molecular Neurophysiology, NICHD, NIH, Bldg. 49, Room 5A-22, 49 Convent Drive, MSC 4480, Bethesda, MD 20892-4480, Phone: 301-496-5493, FAX 301-496-9939, james@helix.nih.gov.

Introduction

Recent discoveries have highlighted the central role that glial cells play in information processing in the nervous system. A series of findings suggest that glial cells may monitor neural activity and respond with propagated signals of their own and may also release chemical gliotransmitters (Araque et al., 1998, Parpura et al., 1994, Robitaille, 1998). Oligodendrocytes and Schwann cells appear to receive input during action potential traffic along the axons they myelinate (Kriegler and Chiu, 1993, Lyons et al., 1994) and astrocytes monitor and modulate neural activity and plasticity (Fellin et al., 2004, Pascual et al., 2005). Glial cells utilize elevations in intracellular calcium ($[Ca^{2+}]_i$) as the principal means of signaling in response to neural activity. These signals appear to be highly localized spikes of $[Ca^{2+}]_i$ as well as propagated $[Ca^{2+}]_i$ waves that encompass the entire cell (Grosche et al., 1999, Porter and McCarthy, 1996). Transmitters released by glia in response to such signaling have recently been found to modulate synaptic transmission in neural networks (Fiacco and McCarthy, 2004, Pascual et al., 2005, Kang et al., 1998). This body of work, however, has to be viewed in the light of a recent finding where selective stimulation of astrocyte Ca^{2+} signals did not affect synaptic activity (Fiacco et al., 2007).

Neuron-glial signaling in isolated brain slice preparations and action potential-initiated $[Ca^{2+}]_i$ signals in isolated nerve preparations have been recorded using potentiometric indicators (Konnerth et al., 1988) and cell-permeant calcium indicator dyes (Hirase et al., 2004), (Kriegler and Chiu, 1993). *In vivo* imaging of glial cell Ca^{2+} signals were also similarly recorded using bulk loading of cells in cortical areas by microinjection of cell-permeant indicator dyes (Wang et al., 2006, Shummers et al., 2008). In all of these experiments, indicator loading into both neurons and glia compromises the resolution of specific neuronal or glial cell signals. While a number of key discoveries have given us a new and exciting view of glial cell participation in plasticity and information processing in the nervous system, much detail needs to be uncovered. These studies are hampered by the lack of discrete Ca^{2+} indicator loading into glial cells. Astrocytes are identified in the brain tissue using co-labeling with sulfarhodamine 101 (SR-101), which is fraught with problems including labeling of neurons in older animals. Discrete labeling of glial cells using microinjection of Ca^{2+} indicators or by patch clamp procedures is also problematic because of damage to the cell. Expressing a genetically encoded Ca^{2+} indicator discretely in astrocytes would provide an ideal system to study astrocytic signaling in the brain both *in vitro* and *in vivo*.

The development of novel Ca^{2+}-sensitive fluorescent proteins offers new approaches to study Ca^{2+} signaling. Miyawaki and colleagues have succeeded in designing calmodulin-based Ca^{2+} indicators that rely on fluorescence resonance energy transfer (FRET) between cyan and yellow fluorescent proteins (CFP and YFP, respectively), including the yellow cameleon (YC) variants (Miyawaki et al., 1997). YC Ca^{2+} indicators, YC 2.1, YC 3.12, and others have been successfully applied in many invertebrate systems (Kerr et al., 2000, Suzuki et al., 2003, Gordon and Dickinson, 2006, Reiff et al., 2005). Attempts to record neuronal activity in the mouse, either in the cortex, (Hasan et al., 2004), hippocampus (Pologruto et al., 2004), or cerebellum (Diez-Garcia et al., 2005) suffered from low signal-to-noise in the measurements. YC 3.60 provides a greatly expanded dynamic range *in vitro* over its predecessors (Nagai et al., 2004). Here we show that transgenic expression of YC 3.60 to record Ca^{2+} signals in glial cells offers a highly effective approach to studying glial responses to neuronal activity. For the first time it is possible to record glial cell Ca^{2+}-based excitability without need for patch clamp procedures or cell injection.

We constructed a transgenic mouse line expressing YC 3.60 directed by a 9.8 kilobase (kb) human S100β promoter. This S100β promoter has been previously used to achieve cell

specific expression of green fluorescent protein (GFP) in Schwann cells and astrocytes in mice (Vives et al., 2003, Zuo et al., 2004). We used this promoter to drive expression of YC 3.60 in astrocytes and Schwann cells, and yield the capability to study population-wide glial cell Ca^{2+} signals *in situ* in response to neural stimulation.

Methods

Transgenic mouse development

A 15.1 kb transgene was constructed using standard molecular techniques described in detail in supplementary methods (Supplementary information). Figure 1A illustrates the 13.9kb pS100β-eGFP vector (Figure 1A-a1, a gift from Dr. Wesley Thompson, University of Texas, Austin, TX), the 7.3kb pCDNA3.1-YC3.60 vector (pCMV-YC, Figure 1A-a2, a gift from Dr. Astushi Miyawaki, RIKEN, Tokyo), and the complete S100β-YC 3.60 transgene (Figure 1A-a3). Briefly, the eGFP cassette in the pS100β-eGFP was removed and replaced with the YC 3.60 cassette from the pCMV-YC 3.60 plasmid. The 1.9kb YC 3.60 cassette from the pCMV-YC 3.60 plasmid was fused downstream of the 9.8kb human S100β promoter with an SV-40 poly-adenylation sequence directly 3' to YC 3.60. The assembled plasmid was amplified, and the derived clones were sequence verified and two, pS100β-YC 3.60-1 and pS100β-YC 3.60-2, were selected for use. Agarose gel electrophoresis verified the expected size of the plasmid (Supplementary Figure 1, see Supplementary information).

The efficiency and cell specificity of transgene expression and the functionality of the trangene product were tested in *in vitro* transfection experiments. The two identical transgene clones, pS100β-YC-1 and pS100β-YC-2 were transfected into S100β-expressing C6 glioma cells, and HEK-293 cells served as non-S100β expressing controls. The details of this experiment and the results are presented in Supplementary information (Supplementary Figure 2).

All animal use conformed to the National Institutes of Health's Animal Care and Use Committee Guidelines and were carried out under the NICHD ACUC approved protocol (Protocol number 04-022). Transgenic mice were generated using standard techniques previously described (Hogan, 1994). Microinjections were performed at the NIMH Transgenic Core Facility. Briefly, C57Bl6/J fertilized oocytes were microinjected with the linear S100β-YC3.60-SV40 gene fragment. Surviving oocytes were transferred into the oviducts of pseudopregnant CD1 females. Progeny were housed at the NICHD animal facility and screened for founders by standard PCR using the forward primer: CCATGCCTGCTGCTCTGAGCTTGA, and the reverse primer: TCGTTGGGGTCTTTGCTCAGGGC. Genopositive founders were set up with wild-type C57Bl6/J mice, and progeny were screened for the transgene in the same fashion and bred to homozygosity. Homozygous mice were identified by using standard backcrossing procedures.

Immunohistochemistry of brain sections

For immunohistochemistry of neonatal brains, pups were sacrificed by decapitation at postnatal day one. Brains were removed and placed in 4% paraformaldehyde for 48 hours at 4°C, rinsed in PBS (pH 7.4) and infused with 30% sucrose at 4°C. Brains were fastened to a −20°C cutting block using OCT. Sagittal 50 μm thick sections were cut using a cryostat (Leica CM 3050 S, Bannockburn, IL), and transferred to SuperFrost Plus slides (Fisher Scientific). They were allowed to dry in the dark, and stored at 4°C. Sections were rinsed in PBS (pH 7.4) at room temperature and blocked for 1 hour in PBS containing 0.3% Triton X-100, and 21% goat serum. They were washed twice in carrier solution (PBS containing 0.3% Triton X-100 and 1% goat serum), and incubated in rabbit anti-GFP antibodies

(Molecular Probes, 1:400) in carrier solution overnight at 4°C. Slides were rinsed again, and incubated in Rhodamine Red-X conjugated goat anti-rabbit secondary antibodies (1:50) for 1 hr at room temperature. After rinsing twice in carrier solution, and once in PBS, they were mounted under cover slips using MOWIOL (Holtzclaw et al., 2002).

For immunohistochemistry of adult transgenic mouse brains, mice were anaesthetized with isoflurane and transcardially perfused with 1xPBS pH 7.4 followed by 30ml of 4% paraformaldehyde. Brains were removed, postfixed at 4°C for 4 hours, and 30μm sections were cut (Neuroscience Associates, Knoxville, TN). They were developed for immunohistochemistry as above using the following antibodies: anti-GFP (1:400), S100β (1:2000, mouse monoclonal, Sigma, St. Louis, MO), GFAP (1:100, mouse monoclonal, Chemicon, Temecula, CA), NeuN (1:1000, mouse, monoclonal, Chemicon), CNP (1:100, mouse monoclonal, Covance, Denver, PA), or NG2 (1:500, rabbit polyclonal, Chemicon). In some cases an Invitrogen mouse monoclonal anti-GFP antibody (1:100) was used. Anti-Iba1 antibody (1:1000) was purchased from Wako Chemicals, USA (Richmond, VA). All mouse antibodies were secondary stained with FITC labeled goat-anti-mouse secondary antibodies. Immunocytochemistry of transfected cells followed the same procedure, except cells were fixed in 4% paraformaldehyde for 10 minutes at room temperature and permeabilized with methanol at −20°C for 3 minutes prior to incubation with primary antibodies (Holtzclaw et al., 2002).

Cells on cover slips and brain sections were imaged on a Zeiss LSM 510 confocal microscope on an Axiovert (inverted). Rhodamine Red-X or FITC staining was excited using a 543nm Helium-Neon laser or a 488nm Argon ion laser, and images were captured using 560nm long pass, or 500–530 band pass filters, respectively. For cell counts from stained tissues, Z-stacks were collected using a 63× Zeiss plan-apochromat oil immersion objective (1.4 NA), or a 40× Zeiss plan-neofluar oil immersion objective (1.3 NA). Optical sections (1μm) were acquired at 1024×1024, 12 bit resolution on a Zeiss 510 confocal microscope on an Axioskop (upright). Cells were counted from three separate 1μm slices spaced 10μm apart along the z-axis. Multiple repeats of each stain and multiple volumes were collected for each cell count. Montages of whole brain were obtained in the same manner, but with a 5× Zeiss plan-apochromat dry objective (0.16NA), or a 10× (0.3NA) objective.

Acutely Isolated Brain slices

Mice were anaesthetized in a CO_2 chamber and immediately decapitated. Brain was removed and placed in ice-cold cutting solution (in mM: NaCl 87, $NaHCO_3$ 25, KCl 2.5, NaH_2PO_4 1.25, $MgCl_2$ 7.0, $CaCl_2$ 0.5, glucose 25.0, sucrose 75, ascorbic acid 0.4). Transverse slices (300–400μm) were prepared from the hippocampus and cortex, and parasagittal slices were prepared from the cerebellum. All slices were cut at 0°C on a vibratome (series 1000, Ted Pella, Redding, CA) in constantly aerated cutting solution. Cut sections were transferred to a recovery chamber containing cutting solution and continuously aerated with 95% O_2 5% CO_2 at 34°C for 1 hour. Sections were then transferred to a custom built recording chamber and perfused with aerated artificial cerebrospinal fluid (ACSF) (in mM: NaCl 125, $NaHCO_3$ 25, KCl 2.5, NaH_2PO_4 1.25, $MgCl_2$ 1.0, $CaCl_2$ 2.0, glucose 25, ascorbic acid 0.4) at 2ml/minute.

To record agonist-evoked Ca^{2+} signals, glutamate (300μM) in ACSF was applied using a picospritzer (IM 300, Narishighe, Japan) through a micropipette (1–3MΩ resistance tip). The micropipette tip was positioned directly adjacent to the field of interest and just outside of the field (see Fig. 6 A) and approximately 100nl of glutamate was ejected by a 20 ms, 10 psi nitrogen puff. Verification of ejection volume was performed prior to the experiments by filling the pipette with Fluo-4 salt solution and using spectrofluorimetric measurements to

ascertain the volume of the puff. For on-line verification of agonist application and removal, the glutamate solution was spiked with 1% (v/v) quantum dot nanocrystals (QD655nm, Quantum Dot Corp, Hayward, CA). Electrical stimulation of hippocampal Schaffer collaterals or mossy fiber pathways was achieved using a custom built bipolar electrode connected to a Stimulus Isolation Unit (WPI, Sarasota, FL) controlled by the Digidata controller and Clampex software (Axon Instruments, Foster City, CA). In each experiment, a one second stimulus train (100 μA, 50 ms, 100 Hz) was applied. A monopolar glass extracellular electrode (3MΩ tip resistance) connected to a Multiclamp headstage with output to Clampex software was positioned near the field of view (300μm away from the stimulating electrode) for recording field potentials.

Brain slices or isolated sciatic nerves were imaged using a Zeiss LSM 510 upright fluorescence microscope (Axioskop, Zeiss Microimaging, Jena, Germany) with 2-photon excitation. In a number of initial experiments a 20× (0.50 NA) water immersion objective lens with a back aperture of 7.5mm was used for imaging. CFP was selectively excited using a tunable Ti-Saphire Chameleon laser (Coherent Inc., Auburn, CA) mode-locked to 805nm, and CFP/YFP emissions were imaged through two separate internal scanned detectors with 435–485nm BP (CFP), and 535–590nm BP YFP) filters. The 805nm IR beam excited CFP exclusively without any spillover excitation of YFP. This was verified using COS cells transfected with CFP or YFP alone, and cultured together on glass cover slips. Excitation with the 805 nm laser line did not excite cells labeled with YFP alone. A third emission path was directed, when needed, to a separate META detector spectrum-locked at 650–660nm to detect QD 655 included in the picospritzer to image agonist application. Images were acquired at 1 to 3 Hz (1.6μs, or 1.9μs pixel dwell times) and agonist or electrical stimulation was applied during image capture. In later experiments, in order to increase signal-to-noise ratios, slices were imaged with a 20× (1.0 NA) water immersion objective lens with 17mm back aperture, and fluorescence emission was collected simultaneously through two non-descanned detectors with 460–500BP (CFP) and 520–600BP filters (YFP). Generally laser power setting varied between 5 and 7%.

In vivo imaging of cortical astrocytic Ca^{2+} signals

Cranial windows were installed above the somatosensory cortex of adult mice (over 60 days old). We used the technique for repeated imaging of the somatosensory cortex in mice developed by the Svoboda laboratory (Gray et al., 2006) as modified by (Mostany and Portera-Cailliau, 2008). Mice were anaesthetized with isoflurane (4% for initial induction) in O2-enriched medical air and when unresponsive to toe pinch, were maintained under anaesthesia with 2% isoflurane. The animal was placed in a custom-built stereotaxic device equipped with plastic ear pieces and a bite-bar. A mixture of Dexamethasone (0.2mg/Kg) and Carprofen (5 mg/Kg) was administered subcutaneously, in order to prevent swelling of the brain and to reduce inflammatory response respectively. The mice were on a heated blanket (Harvard Apparatus, Holliston, MA), which was maintained at 37.4 °C by continuously monitoring the rectal temperature with feed-back to the warming pad.

Surgery was carried out under strict aseptic conditions, and all ARAC guidelines for survival rodent surgery were followed for all procedures. A craniotomy (diameter 3 to 4 mm) was performed above the right somatosensory cortex (center at 2 mm lateral to bregma, 0 mm caudal to bregma, diameter 3 mm), leaving the dura intact. Before removal of the skull, the area was painted with lidocaine and epinephrine to reduce bleeding. A small amount of cyanoacrylate gel was applied all around the edge of the cover glass such that the glass cover slip was glued tightly over the cranial window. Once the glue had dried, dental acrylic was applied throughout the skull surface covering also the small rim of the cover slip. In addition, a titanium bar (0.375×0.125×0.05 inch) was glued to the skull using dental

acrylic. The dental acrylic was allowed to cure for 10 to 15 minutes and the animal was then placed in a warm cage to recover.

For imaging experiments, the animal was again anaesthetized (2% isoflurane) and maintained under 0.75 to 1.0 % such that the animal was very lightly under, and responsive to somatosensory stimuli. The mouse was placed on a custom built animal holder with a stereotaxic head holder. This head holder had a horizontal rod that clamped the titanium bar glued to the skull. The bar was secured to the stereotaxic holder and the entire assembly was mounted under the microscope on a custom built stage. The assembly was adjusted until the cranial window was oriented horizontally under the microscope objective. The well over the cranial window was filled with a few drops of water, and the cortical cells were visualized using a Zeiss 20× 1.0 NA objective with a 17mm back aperture. Two-photon imaging of labeled glial cells was carried out using 805 nm excitation from a Chameleon femtosecond laser and the excitation beam was passed through a precompensation device (Coherent) to ensure optimal excitation efficiency in the two photon mode. Fluorescence emission was collected at 475 nm (460–500nm BP) and 535 nm (520–600nm BP) using two high sensitivity, non-descanned detectors placed just above the objective. Generally, images (512×256) were acquired at 2Hz without averaging and the pixel dwell times were between 1.6 and 1.9 μs. Laser power was set between 10 and 15%. For purposes of field selection, the excitation of YC3.60 labeled cells was viewed by confocal illumination at 488 nm (emission at 525 nm).

Data Analysis

In Ca^{2+} imaging experiments, fluorescence intensity within regions of interest (ROIs) drawn around cell periphery or regions within the cellular space, was measured using LSM (Zeiss Microimaging) or Metamorph (Molecular Devices, Downington, PA) software packages. Fluorescence intensity of the non-zero pixels within each ROI were averaged separately for CFP and YFP emissions and plotted against time. The fluorescence emission ratio was computed on a pixel-by-pixel basis and scaled for image rendering. Numerical data was extracted from the ratio images using the same ROIs and plotted against time using Kaleidagraph software (Synergy Systems Inc, Reading, PA). Peak amplitudes of fluorescence changes were calculated by subtracting averaged baseline emission intensities, and integrated area under a peak was calculated using a standard Trapezoid rule. All still images captured were exported directly from LSM software as full resolution tiff files. All images were brightened, sized, and false-colored/merged identically using Adobe Photoshop. Multiple images obtained from brain sections were rendered as montages. All image renderings followed the guidelines recommended by the Journal of Cell Biology (Rossner and Yamada, 2004).

Results

Generation of transgenic mice

Transgenic C57Bl6/J mice were generated by standard microinjection techniques (Hogan, 1994). PCR analysis of genomic DNA from F1 generation mice showed that the transgene had been integrated into the genomes of nine germ line-transmitting founders. To verify expression of the transgene product and identify the expression pattern of YC 3.60, a newborn F1 litter from each founder line was sacrificed, and sagittal cryostat sections (50 μm thick) were prepared for fluorescence-based immunohistochemistry using anti-GFP antibodies and for imaging native fluorescence of YC 3.60. A F1 mouse brain from one of the transgenic lines shows brightly stained astrocytes (Figure 2B). Native fluorescence in YC 3.60 expressing cells was imaged in a similar cryostat section from another new-born transgenic mouse without immunohistochemical staining. Brightly fluorescent cells, but

fewer in number were visible without staining (Figure 2A). This initial screening revealed four transgenic lines, which showed significant cellular expression of product in astrocytes in brain regions and Schwann cells in peripheral nerves.

Vibratome sections of whole brain and isolated teased sciatic nerves were used to assess levels of YC 3.60 fluorescence without immunohistochemical staining. For this second screening step, we selected three of the transgenic lines that showed the highest levels of expression. Table 1 outlines the degree of labeling observed in the different brain regions. In most lines, intrinsic fluorescence due to YC 3.60 expression could be readily imaged (++ to ++++, Table 1), while in some, transgene expression is detectable only after immunohistochemical staining with anti-GFP antibodies (+, Table 1). This analysis revealed that two of the four transgenic lines showed intense staining in most of the brain regions, which can be imaged using one and two-photon microscopy. One of the four lines (line 2622, Table 1) showed very low cellular fluorescence levels that precluded imaging at low light level and was therefore discarded. The fourth line showed robust YC 3.60 expression in Schwann cells in peripheral nerves (sciatic nerve, Figure 2F) and no intrinsic fluorescence in astrocytes in the brain. Transgene expression in astrocytes could be observed after immunohistochemistry using anti-GFP antibodies. This line was named S100β-YC-P for its cell-specific expression of YC 3.60 in all Schwann cells in the peripheral nervous system (line 2562, Table 1). Two-photon excitation revealed that fluorescence was restricted to Schwann cell cytoplasmic compartments, Cajal bands in the paranode at the nodes of Ranvier, incisures, and Schwann cell soma (Figure 2F). One of the two transgenic lines with significant YC 3.60 expression in different brain areas showed very high levels of fluorescence in cerebellar Bergmann glial cells (Figure 2C), and bright fluorescence in populations of cells with glial morphology in the hippocampus and other brain regions. This line was named S100β-YC-C (line 2547, Table 1). A third line of mice, S100β-YC-B, showed brighter fluorescence than S100β-YC-C in glial cells within most regions of the brain, albeit in small number of cells (line 2604, Table 1). The S100β-YC-P transgenic line was set aside for future studies on Schwann cell signaling and axonal-glial communication. In this study, the two lines with YC 3.60 expression in brain regions, S100β-YC-C, and S100β-YC-B, were further characterized and glial cell signals *in situ* were recorded in isolated brain slice preparations. The S100-YC-C line was bred to homozygosity, but we did not succeed in obtaining homozygous animals with the S100-YC-B line. Both S100β-YC-C, and S100β-YC-B lines of mice showed significant YC 3.60 expression sufficient to provide recordings with good signal-to-noise in two–photon microscopy using isolated brain slice preparations or *in vivo* recordings. The S100-YC-C line of mice expressed YC 3.60 in a larger percentage of S100β-positive astrocytes in most of the brain areas, and therefore is a more preferable model.

YC 3.60 expression in the transgenic mice

Sagittal sections (30 μm) were prepared from adult mouse brains from both S100μ-YC-C, and S100β-YC-B lines and developed for immunohistochemistry using cell-specific marker antibodies and anti-GFP. These dual-staining experiments revealed YC 3.60 expression throughout the brain in both transgenic mice, but the intensity of staining and proportion of cells with GFP staining varied between the different brain areas. In all brain regions, numerous cells with astrocyte-like morphology were seen in the two transgenic mice. The cumulative results are summarized in Tables 2 and 3. The major difference between the two lines of transgenic mice was the number and intensity of staining in astrocytes (see Table 3). In the brains of S100β-YC-C line, GFP-containing cells were more numerous, compared with mice from the S100β-YC-B line. The staining intensity, and intrinsic CFP-YFP fluorescence, however, were more intense in the latter. While astrocytes were the predominant cell type that contained GFP immunoreactivity, there were a number of GFP-

positive cells that did not stain for S100β in both lines of mice. Antibodies against the cyclic nucleotide phosphodiesterase (CNP), a marker for cells of the oligodendrocyte lineage (Sprinkle, 1989, Gravel et al., 1998), stained GFP-positive cells in all the brain regions tested (Table 2). Similarly, cells stained by antibodies against Iba1, an antigen exclusively found in microglia, also showed GFP immunoreactivity (Imai et al., 1996, Ito et al., 1998). These results suggested that the S100β promoter-directed transgene expression was not exclusive to astrocytes. Since the different cell types could not be readily identified by morphological criteria, unequivocal identification of cells would require additional strategies. However, the transgenic mice developed in this study provide the opportunity to record glial cell Ca^{2+} signals in isolated brain slices as well as anaesthetized mice.

YC 3.60 expression in the hippocampus

In the hippocampus of adult mice from the S100β-YC-C line, 51.8±10.3% of S100β positive cells showed GFP staining (Table 3), and this represented the majority (99.1±1.8%) of all GFP-containing cells (Table 2). In the S100β-YC-B line, however, only about 22% of S100β-positive cells expressed YC-3.60, and this represented 79% of all GFP-containing cells (Table 2, and 3). In both lines of mice, YC 3.60-positive cells were morphologically identifiable as astrocytes (Bushong et al., 2002, Matthias et al., 2003). Cells with large spongiform process arbors as well as smaller cells containing YC 3.60 were observed (Figure 3A and B). Many of these cells had elongated cell somas with multiple large branches radiating parallel or perpendicular to those of their neighboring glia. Numerous YC 3.60-positive astrocytic processes extended to wrap small blood vessels (Figure 3B, arrow), and YC 3.60 expression was found in the cell soma, and processes in astrocytes (Figure 3). Figure 3B shows a maximum intensity projection of one protoplasmic astrocyte in CA1 *stratum radiatum* with the cell body and all processes filled with YC 3.60 immunoreactivity. 3D animation of this dataset (Supplementary Figure 3) reveals the astrocytic end feet enwrapping a blood vessel. A number of the dual stained cells throughout the hippocampus appeared identical to the lucifer yellow filled protoplasmic astrocytes described by (Bushong et al., 2002, Bushong et al., 2003, Matthias et al., 2003) and YC 3.60 staining filled the fine spongiform processes. In sections obtained from brains of S100β-YC-B mice, GFP-containing cells were less numerous, but were significantly brighter (see Table 2, and 3).

There were a number of FP-immunoreactive (Fluorescent protein-immunoreactive) cells in the hippocampus that did not stain for S100β (23.6%, Table 3). Furthermore, anti-CNP stained cell bodies in the dentate gyrus (DG) and CA3 pyramidal cell region. Colocalization of GFP and CNP was observed in 29.2±5% of 56 CNP positive cells (arrowhead in Figure 3D). Table 2 summarizes the cell count data from all dual labeling experiments. In the sections dual stained for CNP and GFP, approximately 59% of all cells counted stained for GFP alone and did not show colocalization with CNP in the S100β-YC-C mice. CNP-positive cells expressing YC 3.60 were smaller than S100β-positive cells, and usually had round to slightly oblong cell bodies with few processes (arrowhead in Figure 3D). YC 3.60 was rarely seen in CNP-containing myelinated fiber tracts in the corpus callosum (CC) or the dentate gyrus. Similar results were obtained in dual staining experiments using an antibody against the proteoglycan NG2 (data not shown) with 28.8±7.9% of NG2-containing cells showing GFP immunoreactivity, and 59.7% of cells being NG2-negative, but GFP-positive. Staining for the neuronal nucleus marker NeuN specifically marked cell bodies in *stratum radiatum* and cells in the surrounding pyramidal cell layer. None of these neuronal profiles, however, stained for GFP (Figure 3E, Table 2).

YC 3.60 expression in the cerebellum

By far, the largest number of GFP-positive cells were found in the cerebellum, compared with other brain regions, in the brains of both transgenic lines. In the S100β-YC-C line, dual

staining with anti-S100β and anti-GFP antibodies showed 78.5±7% of S100β positive Bergmann glial cells expressed YC 3.60 (139 cells, Figure 3 F–J, Table 3). Staining in Bergmann glial cells was intense in the cerebellum of mice from the S100β-YC-B line. The number of stained cells, however, was significantly less compared with S100β-YC-C brains. In the cerebellum, most of the GFP-positive cells were also S100β-positive (69.1% see Table 2), and no GFP-containing Purkinje neurons were observed (see Figure 3J). Bergmann glial cells showed prominent staining with anti-GFP antibodies with uniform staining in the soma and all the major processes. Most of the Bergmann glial cells showed very high levels of GFP staining including in the fine terminal processes (Figure 3G). CNP and NeuN-positive cells were found in the granule cell layer, but only few of these cells contained GFP immunoreactivity (Figure 3J, Table 2). In the granule cell layer, YC 3.60-expressing (GFP positive) astrocytes were occasionally observed in both transgenic mice (data not shown).

YC 3.60 expression in other brain regions

In the cortex, dual staining showed that 60% of 192 S100β-positive cells were immunopositive for YC 3.60 in S100β-YC-C mice (Figure 4A, Table 3). This amounted to approximately 67% of the GFP-positive cells containing S100β immunoreactivity (Table 2). A few cells containing GFP immunoreactivity did not contain S100β (21.9±5.69%). Dual staining for CNP and GFP, or NG2 and GFP, showed that significant numbers of CNP-positive cells contained GFP immunoreactivity (Table 2), and were morphologically similar to oligodendrocyte progenitor cells (OP cells, Figure 4B). Such GFP-containing cells were found primarily in layer IV cortex and throughout the CC. CNP-positive myelin in the CC contained no YC 3.60, and none of the NeuN-positive cell bodies showed YC 3.60 expression anywhere in the cortex (Figure 4C, Table 2). A significant proportion of Iba1-positive microglia were also found to contain GFP immunoreactivity (Table 2).

In the olfactory bulb, 81.3±5.02% S100β-positive cells were GFP-positive (Figure 4D), and 50.4±13.0% of CNP-positive cells were also GFP-positive (Table 3). While these cells possessed distinctly astrocytic or OP cell morphologies, they expressed YC3.60 only weakly. None of the NeuN-positive cell bodies contained YC 3.60 (Table 2).

In the brain stem, unique YC 3.60 expression was observed in cell bodies and axons in NeuN-positive large motor neurons in the S100β-YC-C mice (15±1.6% of 99 NeuN positive cells, Figure 4I). This amounted to approximately 30% of GFP-positive cells (Table 2). In S100β-YC-B mice, 47% of GFP-containing cells contained NeuN stained nuclei (Table 2). These neurons were morphologically distinct with extremely large soma with NeuN-positive nuclei. GFP-expressing large motor neurons amounted to 11.1% of all cells counted. In the brain stem, approximately equal number of astrocytes and OP cells were positively stained with GFP antibodies (Figure 4G, and H). Cell counts showed that, in both transgenic mouse lines, about 60% of S100β, and CNP-positive cells stained for GFP. The fine terminal processes of the cells of the oligodendroglial lineage did not stain for YC 3.60.

Glutamate evoked glial cell Ca^{2+} signals *in situ*

In order to verify that the YC 3.60 within cells was functional as a Ca^{2+} indicator *in situ*, we used isolated, acute brain slice preparations, and previously characterized experimental paradigms to elicit neurotransmitter-induced, glial cell Ca^{2+} signals. Astrocytic Ca^{2+} signals in response to exogenously applied glutamate have been demonstrated by a number of laboratories (*see for review:* (Schipke and Kettenmann, 2004). A 100 nl puff of 500 μM glutamate in ACSF, applied through a glass pipette (1–3MΩ resistance) positioned directly over the field under superfusion (Figure 5A), elicited increases in the YFP/CFP fluorescence ratio in majority of the cells examined (Figure 5A–C). Figure 5B shows the Ca^{2+} response from one cell in the field (Figure 5A, box). Glutamate addition caused an immediate large

increase in YFP/CFP ratio indicating the large spike in Ca^{2+} concentration in the cell, as verified by the reciprocal change in CFP/YFP fluorescence intensity (Fig. 5B). After this initial Ca^{2+} spike, the glutamate application elicited a series of what appeared to be spontaneous Ca^{2+} rises until recording ended (See Fig 5B). In nine different slice preparations obtained from heterozygous (3 slices) or homozygous (6 slices) S100-YC-C mice, (14 trials) 65% of the cameleon-expressing astrocytes in the microscopic field (20×, 0.6 NA, or 20× 1.0 NA objectives) responded to the glutamate puff (n=136 cells). The average glutamate-induced YFP/CFP ratio change was 68±22%. In most experiments, one or two cells showed very large YFP/CFP ratio changes (>100%) compared with the rest, and some cells did not respond at all (Figure 5A and C). The largest response recorded was a 312.8% change in the YFP/CFP ratio in a field where all the cells examined showed an average response of 112±32%. These recordings of astrocytic Ca^{2+} signals in the brain slice preparation with the YC 3.60 cameleon are comparable in amplitude and signal-to-noise to those previously recorded using Ca^{2+} sensitive dyes such as Fluo-4 or calcium green (Porter and McCarthy, 1995, Duffy and MacVicar, 1995, Araque et al., 1998). Thus the YC 3.60 cameleon expressed in astroctyes provides remarkably good signal-to-noise in measurement of cellular Ca^{2+} signals *in situ*. This is in sharp contrast to previous experiments using yellow cameleons in transgenic mice, where the largest reported signal amplitudes are in the range of a <10% change in YFP/CFP ratio during cellular stimulation (Hasan et al., 2004), (Pologruto et al., 2004, Diez-Garcia et al., 2005).

YC 3.60 fluorescence extended into the entire process arborizations of astrocytes. During rest, the cell soma were easily visualized, and the finer processes appeared as a hazy cloud above background levels of fluorescence in the field. Upon stimulation, however, we were able to measure increases in the fine process fields surrounding astrocyte soma. YFP emission increased, while CFP emission decreased (data not shown). Similar increases in the YFP/CFP ratio in dimly fluorescent cellular process arbors were observed in 8 of the 14 experiments with an average rise in YFP/CFP ratio fluorescence of 49±6% over resting levels. These observations suggested that networks of astrocytic fine processes containing extremely low levels of YC 3.60 were reporting glutamate-evoked Ca^{2+} signals. The histogram (Figure 5C) shows a frequency distribution of response amplitudes (535/480 nm emission ratio) recorded in cortical astrocytes, and demonstrates the usefulness of the YC 3.60-expressing transgenic mice for measuring cellular Ca^{2+} signals *in situ*.

In another set of experiments, we examined Bergmann glial cells in cerebellar slices obtained from heterozygous S100-YC-C mice (Figure 5D–F). Application of a puff (100nl) of glutamate over Bergmann glial cells elicited increases in YFP/CFP fluorescence ratios indicating cellular Ca^{2+} rises. The peak amplitude of these signals was 57.5±28.8% (n=12), which was significantly lower than those recorded in astrocytes in cortical or hippocampal slices. In these experiments, we spiked the agonist-containing solution with 1% v/v Quantum Dots (QD 655nm, Quantum Dot Corporation, Hayward, CA), which allowed for precise temporal monitoring of agonist delivery to slices (Figure 5E, F). Glutamate application to the Bergmann glial cell body evoked reproducible Ca^{2+} oscillations. The small delay in the Ca^{2+} response of the cell upon glutamate addition is due to the low concentration of glutamate in the pipette and the low injection volume (100 nl). Furthermore, the slice was under constant perfusion with ACSF with the pipette placed over the slice. Application of glutamate on glial cell processes alone caused Ca^{2+} responses in only small domains of the processes (data not shown). Localized Ca^{2+} signals in microdomains of Bergmann glial processes have been recorded using the Ca^{2+} indicator dye, Oregon Green (Grosche et al. 1999). These authors concluded that such microdomains of Ca^{2+} signaling represented glial cell processes in close association with parallel fiber synapses. Despite differences in the stimulus paradigms, the characteristics of Ca^{2+} signals

recorded from Bergmann glial cells in their study and in the transgenic mouse brain slices in this report were remarkably similar in amplitude and duration.

Ca^{2+} signals evoked by neuronal stimulation in astrocytes *in situ*

Stimulation of Schaffer collaterals in hippocampal slices evokes robust Ca^{2+} signals in astrocytes in the *stratum radiatum*, and *stratum moleculare-lacunosum* (Dani et al., 1992, Porter and McCarthy, 1995). These astrocytic Ca^{2+} signals are most likely due to synaptically released glutamate, which stimulates metabotropic glutamate receptors on astrocytes to evoke a Ca^{2+} response (Dani et al., 1992, Sul et al., 2004), (Jabs et al., 2005). Astrocytes in turn coordinate long-term potentiation and depression through the modulation of extrasynaptic ATP concentrations (Pascual et al., 2005). A recent report showed that astrocytes also affect synaptic scaling by releasing TNF-α (Stellwagen and Malenka, 2006). Figure 6A shows a field of CA1 *stratum radiatum* astrocyte cell bodies and processes imaged using two-photon excitation. Stimulation of the Schaffer collateral pathway (arrow in Figure 6B, 100 μA pulses at 50 Hz, 0.5ms pulse width, for 1s) caused an immediate Ca^{2+} rise in two astrocytes in the field (marked 1 and 2). The response in cell 1, shown Figure 6B, was immediate and robust. In addition, this cell shows continued low amplitude spontaneous activity following the stimulation throughout the recording period. The single wavelength traces in color show the appropriate reciprocal changes in YFP and CFP fluorescence intensities corresponding to the evoked and spontaneous Ca^{2+} rises. Similar reciprocal changes in YFP/CFP fluorescence intensities were monitored in each case to verify that increases in ratio were not due to unequal photobleaching or movement artifacts, and were indeed due to Ca^{2+}-induced increase in FRET. The applied stimulus train (Figure 6C), and the very first field potential (Figure 6D) recorded in response, are shown.

In ten different slice preparations (16 experiments) from S100-YC-C and S100-YC-B mice, the stimulus-evoked YFP/CFP ratio increase occurred in 76.8±12% of 80 cells, and in each case extracellular field potentials were recorded. The largest fluorescence increase recorded was a 222% change in the YFP/CFP ratio, and the average response from all 12 trials was 67.8±21%. Similar stimulus-evoked Ca^{2+} responses were repeated multiple times in the same field, and were completely abolished by bath application of tetrodotoxin (1=M, data not shown). A similar experiment is presented as an animation of time lapse recording in Supplementary Figure 4 (see Supplementary information). These Ca^{2+} signals recorded in response to hippocampal stimulation in YC 3.60 expressing mouse tissues were comparable to similar recordings using Ca^{2+} indicator dyes in previously published studies (Dani et al., 1992, Perea and Araque, 2005).

Electrical stimulation-evoked Ca^{2+} signals were also recorded in cerebellar slice preparations. Ca^{2+} signals in Bergmann glial cells have been previously elicited by stimulation of the parallel fiber pathway or direct stimulation in the granule cell layer (Grosche et al., 1999, Kulik et al., 1999). We utilized this experimental paradigm to investigate electrically-evoked Bergmann glial Ca^{2+} signals in cerebellar slices from S100-YC-C mice. A 1s stimulation (50 Hz, .5ms pulse width, 100 μA) was used in all experiments, which evoked Ca^{2+} rises in distinct domains of Bergmann glial processes. Parallel fiber stimulation elicited Ca^{2+} signals in 60% of Bergmann glial processes examined (n=5). The average response amplitude was 57.6±12.9%. Direct stimulation in the granule cell layer similarly caused Ca^{2+} responses in 5 of 9 Bergmann glial cells (2 slices), with an average response amplitude of 26.5±17.6%. The histogram (Figure 6E) shows a summary of electrical stimulation-evoked Ca^{2+} responses recorded in astrocytes and Bergmann glia and attests to the performance of the transgenically expressed YC 3.60 as a Ca^{2+} indicator in glial cells *in situ*.

Resolving Localized astrocytic Ca^{2+} signals

Immunohistochemical analysis of brain sections from S100-YC-C mice revealed protoplasmic astrocytes that showed high levels of YC 3.60 expression throughout their cell body and spongiform processes (Figure 3B). In most acute slices examined from S100-YC-C or S100-YC-B mice, similar morphologically distinct astrocytes could be identified in the hippocampus. We focused on these large spongiform astrocytes (Figure 7A and B). Two such protoplasmic astrocytes are shown with a brightfield overlay of the fluorescent image (Figure 7A). In Figure 7B, the two-photon image of YC 3.60 fluorescence by itself is shown to highlight the two cells in the CA3 region and cells or portions of cells with different smaller morphological appearance. The stimulating electrode in the hilar region and the recording electrode in the CA3 pyramidal cell dendrites can be seen in the bottom right and upper middle of the figures, respectively (arrowheads). Mossy fiber stimulation has been shown previously to reproducibly elicit Ca^{2+} signals in glia in the CA3 pyramidal layer (Dani et al., 1992). A 1s stimulation (50 Hz, .5ms pulse width, 100 μA) applied while examining the field under low magnification elicited an average fluorescence ratio increase of 51.1±2.8% in both protoplasmic astrocytes. Also, of the 8 other cells in the field in Figure 7B, 6 responded with an average ratio change of 49.6±14.8%.

We then focused on one of the spongiform protoplasmic astrocytes using high magnification objectives and electronic zoom (box in Figure 7B, high resolution in 7C). The stimulus paradigm was repeated during two-photon imaging and YC 3.60 fluorescence changes were measured within the indicated ROIs (Figure 7C). In the cell soma (ROI labeled CB), a large increase in YFP/CFP ratio followed the stimulus (arrow, Figure 7D). Figure 7E, shows the first five field potentials recorded at the CA3 dendrites. ROIs 1 to 7 (Figure 7C) indicate small regions of the cellular process arbors where measurements were made and traces are shown in Figure 7F. Many of these regions represent glial microdomains within the amorphous spongiform morphology of the cell. ROI 7 represents a terminal branch of the astrocyte closest to the stimulating electrode and shows the stimulus-evoked Ca^{2+} increase first. ROI 1 is the farthest away from the stimulus electrode and shows the response last. Thus the cellular Ca^{2+} response elicited by the neural stimulation spreads as a wave through the cell. The small delay in response (2 to 5s) after the stimulus is most likely due to network activation and transmitter release at synapses ensheathed by the astrocyte. Such astrocytic Ca^{2+} responses to electrical stimulation of mossy fiber pathway are blocked by MCPG (20 μM), a metabortopic glutamate receptor antagonist, and by TTX (1 μM) (data not shown). The second protoplasmic astrocyte in the field of view (Figure 7A and B) showed a similar response to stimulation with a fluorescence increase of 32.22% (not shown), but was not further analyzed. In six other hippocampal slice preparations, identical results were obtained with an average cell soma Ca^{2+} response amplitude of 69.1±16.2%. Stimulation evoked either a single Ca^{2+} wave propagating through the cell, or multiple oscillatory waves. Another example of spongiform astrocyte in the hippocampus imaged in a slice is shown in Supplementary Figure 5.

In the hippocampal and cerebellar slices that we examined, a number of astrocytes were spontaneously active, presumably due to existing network activity in the slice (see Figure 5B, 6B and 7F). Figure 7 G and H show an example where we recorded spontaneous activity without any applied stimulus. In 5 such experiments, we were able to record large spontaneous Ca^{2+} transients in 2 slices, often in multiple cells. Spontaneous activity was not always coupled in cells in the same field of view (Figure 7H). This data showed that YC 3.60 within astrocytes is able to faithfully track even very small amplitude Ca^{2+} events (see also Figure 6B). Similar spontaneous Ca^{2+} signals were recorded previously in astrocytes within hippocampal slices using calcium green as Ca^{2+} indicator (Nett et al., 2002)

Ca^{2+} signals in cortical astrocytes recorded in mice *in vivo*

Two-photon imaging is ideal for imaging activity of cells deep within the brain tissue (up to 700 μm in depth) in living animals, and this technique has been repeatedly used by a number of investigators to record astrocytic Ca^{2+} signals in living rodents and ferrets (Takano et al., 2005, Wang et al., 2006, Shummers et al., 2008). These studies utilized synthetic Ca^{2+} indicators which were bulk loaded into cells, and astrocytes were identified using a second cell-specific dye with a longer wavelength emission spectrum (SR101). Since the transgenic lines in this study, S100-YC-C, and S100-YC-B express the encoded Ca^{2+} indicator mostly in astrocytes, we were able to record glial cell activity due to sensory stimulation in the brains of mice from these two lines. We took the approach of implanting chronic cranial windows in mice for repeated imaging of the same animal, and took advantage of methods developed by Svoboda et al (Gray et al., 2006, Holtmaat et al., 2006) with the modifications by (Mostany and Portera-Cailliau, 2008). This method allows for repeated imaging after the surgical wound has completely healed, and for imaging while the animal is under very low levels of (<1%) isoflurane anaesthesia such that cortical activity is not inhibited. Cranial windows were established as described under Methods, and after at least a three week recovery, mice were re-anaesthetized for imaging. This experimental set up allowed us to image YC 3.60 labeled glial cells up to a depth of approximately 300μm within the somatosensory cortex (see Supplementary Figure 6). A pair of fine (27 gauge) needle electrodes was placed under the forepaw skin, and stimulus trains (2 Hz, 1 ms, 2mA, 3s) were applied during imaging YC 3.60-containing astrocytes in layer 2/3 of the somatosensory cortex. Figure 8 shows results of one such experiment, where cortical astrocytes were readily visualized under 2-photon excitation with very good signal-to-noise ratios. Image in figure 8A shows the entire microscopic field visible through the cranial window using the 20× (1.0 NA) objective lens. The left portion of the field is in focus with two-photon excitation compared with the right side of the field where faint outlines of astrocytes are seen. The middle of the field is far from the focal plane. Since the cortical area available for imaging through the window is limited, the same field may be repeatedly imaged. The figure shows a field of astrocytes in the 2-photon focal plane. The differences in fluorescence intensities between the different cells are more than likely due to differences in the depth at which the cells are located in the neuropil, with the cells in focus appearing brightest. Immediately following the stimulus, astrocytic Ca^{2+} signals were seen in a number of adjacent astrocytes in a line, possibly connected in a network. The amplitude of the Ca^{2+} response was significantly higher in those cells in or near the focal plane compared with dimmer cells (ROIs 1, 2, and 3, Figure 8A). Figure 8B shows the individual traces from each astrocyte. Examination of the single wavelength data shows that the increase in ratio is due to a *bona fide* increase in FRET between CFP and YFP (Figure 8C). Similar results were recorded on more than four different trials, and another such experiment is shown as an animation in Supplementary Figure 7. The amplitude and signal-to-noise of recordings were comparable to those made with Ca^{2+} indicator dye loading in astrocytes in somatosensory cortex of anaesthetized mice (Wang et al., 2006). These observations demonstrate the utility of the two transgenic mouse lines developed in this study in imaging astrocytic responses discretely in the cortical areas in living anaesthetized mice.

Discussion

We have developed transgenic mouse lines expressing the YC 3.60 cameleon, a Ca^{2+} indicator under the control of the S100β promoter, which resulted in robust YC 3.60 expression in predominantly astrocytes in the central nervous system and Schwann cells in the peripheral nervous system. This cell-specific expression of the indicator enabled us to record glial cell Ca^{2+} responses evoked by neural stimulation in isolated brain slice preparations. Furthermore, the dynamic range of the YC 3.60 response allowed for Ca^{2+}

measurements in glial cell processes associated with evoked and spontaneous neural activity.

Unlike the early YC cameleons (e.g. YC 3.12), YC 3.60 has been shown to provide 5 to 6 fold larger dynamic range, enhanced signal-to-noise ratios and perform better in intact tissue and whole animal experiments in transgenic animals (Nagai et al., 2004). YC 3.60 was shown to faithfully report neuronal Ca^{2+} transients in hippocampal slice preparations in response to tetanic stimulation. However, when expressed in the CNS, the dynamic range of YC 3.60 was reduced possibly due to generalized expression in all cells since the expression was achieved under the control of the actin promoter (Nagai et al., 2004). The use of the 9.8 kb human S100β promoter in the present study restricted expression predominantly to astrocytes in the brain, and allowed us to reliably record glial cell Ca^{2+} signals with dynamic range and signal-to-noise comparable to previous studies using chemical dye Ca^{2+} indicators. Thus YC 3.60 targeted to non-neuronal cells appears to provide an excellent model for measurement of glial cell activity patterns *in situ*, in tissues as well as in living mice. While targeting YC cameleons to neurons has not been a resounding success (Hasan et al., 2004, Nagai et al., 2004), at least YC 3.60 may be a very useful tool to measure activity patterns in cell ensembles (see also (Reiff et al., 2005)). In addition, the problem of pH-dependent fluorescence changes with early camelons have been adequately addressed by the amino acid changes within the YFP in YC 3.60. The improved photostability, and brightness characteristics renders YC 3.60 a highly desirable, genetically encodable Ca^{2+} indicator currently available to investigate non-neuronal cells. Recently, during the course of this work, new encodable indicators with higher fluorescence quantum yields and using Ca^{2+} sensors other than calmodulin have been designed (Heim and Griesbeck, 2004, Reiff et al., 2005). One of them, Cer-Tn-L15, which uses the chicken troponin-C as the Ca^{2+} sensor promises to be far superior to YC 3.60 as a encodable *in vivo* Ca^{2+} indicator (Heim and Griesbeck, 2004, Mank et al., 2006, Heim et al., 2007).

In the transgenic mouse lines, we found YC 3.60 expression in cells in which the S100β protein itself is reportedly found in astrocytes, Schwann cells, some OP cells in the brain, and some neurons in the brain stem. These results are identical to findings in previous reports on expression of eGFP under the control of the S100β promoter (Vives et al., 2003, Zuo et al., 2004). Furthermore, similar to these previous studies using eGFP and YFP (Hachem et al., 2005, Zuo et al., 2004), we too found considerable variegation in cell-specific expression such that while some S100β-containing astrocytes expressed the transgene product, some others did not. We also found cells expressing the cameleon YC 3.60 that did not contain S100β immunoreactivity (Figure 3c and 4A). This type of variegation, however troubling, afforded one distinct advantage in imaging cellular activity, since it enabled imaging a small number of identified cells (e.g. astrocytes) discretely without fluorescence spill over from neighboring cells. The mice described here could be used to investigate astrocytes in distinct regions of the brain. Variegation in expression of the transgene product such as observed here, while common in transgenic lines (Vives et al., 2003, Zuo et al., 2004, Hasan et al., 2004), is not fully understood. It is frequently attributed to the potential variability in the site of transgene integration causing position dependent effects. In one of the transgenic lines, YC 3.60 expression was robust in Schwann cells in peripheral nerves compared with any other tissue. This type of variegation, which provides unique expression in selected cell populations, might provide a means to genetically target the same cells by reproducibly identifying and utilizing the transgene's integration locus.

A number of recent studies have shown that astrocytes with distinct morphological, molecular and functional characteristics exist in the brain (Bushong et al., 2002, Matthias et al., 2003, Wallraff et al., 2004, Zhou and Kimelberg, 2001). Of the two major types of astrocytes found in the hippocampus, one possessed excitatory amino acid receptors and the

other excitatory amino acid transporters in a mutually exclusive fashion (Matthias et al., 2003), (Wallraff et al., 2004). Subpopulations of the former were found to express AN2, the mouse homolog of NG2 proteoglycan, a marker assigned for OP cells. The GluT type of astrocytes resemble the cells with the spongiform morphology described earlier in dye injection studies (Bushong et al., 2002). In another study, S100β promoter-directed eGFP expression was also observed in CNP-expressing OP cells (Hachem et al., 2005, Vives et al., 2003), and the YC 3.60 expression in CNP-positive cells that we observe here is similar to these earlier observations. Since we found YC 3.60 expression in large protoplasmic astrocytes as well as astrocytes with smaller cell soma (Figure 8), it is possible that transgene expression is not unique to one distinct type of astrocytes in the hippocampus. Indeed, the immunohistochemical analysis of transgenic mouse brains showed that the pattern of YC 3.60 expression closely resembled the pattern of expression of S100β. The expression pattern was similar to eGFP expression in transgenic mice targeted by the S100β promoter (Vives et al., 2003, Zuo et al., 2004, Hasan et al., 2004). A Ca^{2+} indicator protein expressed in this manner would be valuable to investigate differences in cellular Ca^{2+} signaling between the different types of astrocytes found in the brain (Bushong et al., 2002, Matthias et al., 2003).

The objective of this study was to produce mice that will enable measurement of Ca^{2+} signals in astrocytes and Schwann cells *in situ* in isolated tissues and intact animals *in vivo*. We demonstrate here that in these transgenic lines adequate levels of YC 3.60 expression exist and allow for dynamic measurement of cellular activity. We were able to record from subpopulations of protoplasmic astrocytes in the hippocampus and resolve Ca^{2+} signals in single astrocytes as well as discrete cellular regions (Figure 7). In addition, astrocytic Ca^{2+} signals could be recorded in the cortex of live mice under low levels of anaesthesia in response to sensory stimulation of the forepaw (Figure 8). In astrocytes, YC 3.60 fluorescence was bright enough in both S100-YC-C and in S100-YC-B lines, but required high sensitivity, non-descanned detectors to obtain adequate signal-to-noise in measurements. These results are similar to observations in transgenic drosophila lines where a number of genetically encoded Ca^{2+} indicators were compared (Reiff et al., 2005). Furthermore, these signals were similar in amplitude and signal-to-noise to recordings *in situ* and *in vivo* made previously using organic Ca^{2+} indicators such as Fluo-4 (see for example (Porter and McCarthy, 1995, Duffy and MacVicar, 1995, Wang et al., 2006). Our experiments were carried out in both heterozygous and homozygous mice. With calmodulin-based cameleons such as YC 3.60, the low level of expression may be a benefit by reducing Ca^{2+} buffering effects previously observed when cameleons were expressed in tissues using viral vectors as targeting tools (Hasan et al., 2004, Nagai et al., 2004).

While transgene expression was found in most S100β-containing cells, not all such cells contained the YC 3.60 protein. Furthermore, in both lines, expression was observed in cells containing NG2, or CNP (cyclic nucleotide phosphodiesterase), which are markers for the oligodendrocyte progenitors. Transgene expression was also observed in Iba1 antigen-containing cells, which are classified as microglia. This data is similar to observations in eGFP transgenic mice observed in previous studies (Vives et al., 2003, Hasan et al., 2004). Expression in cells which appear to be non-astrocytic might reflect the possible expression of S100β during lineage progression of these cells. This non-astrocytic expression of YC 3.60 was similar in both S100-Y-C-C and in the S100-Y-C-B line of mice (see Table 2). However, in the latter, overall number of astrocytes expressing the transgene was lower. In the cerebellum, few if any non-astrocytic cells were found to express YC 3.60, and the most prominent Bergmann glial cells were readily recognized. Astrocytes in the hippocampus have unique and elaborate morphologies and are thought to establish exclusive territories where they interact with the synaptic neuropil and other glial cells (Bushong et al., 2002, Bushong et al., 2003, Matthias et al., 2003). In the fine process arbors of the protoplasmic

astrocytes in the hippocampus could be recognized by their YC 3.60 fluorescence and Ca^{2+} signals in response to stimulation as well as spontaneous activity could be recorded (See Figure 7). Recordings of astrocytic Ca^{2+} signals in vivo in response to sensory stimulation showed that signals followed a particular spatial pattern, which might suggest territories of astrocytic endowment in the neuropil. Our experience with the transgenic mouse lines generated in this study (S100-Y-C-C, and S100-Y-C-B) suggested that both lines allow for recordings of astrocytic Ca^{2+} signals *in vivo*, and in isolated brain slice preparations using two-photon microscopy. Unequivocal cell identification, however, would require additional experimental strategies.

Cameleons in general have not been well received as highly useful, genetically encodable Ca^{2+} indicators. Recently, however, this deficit has been addressed by the development of the YC series of cameleons and three of them (YC 3.12, YC 3.3, and YC 3.6) were previously shown to be reliable indicators of physiological activity *in situ* (Hasan et al. 2004; Nagai et al. 2004). The performance of YC 3.60 when expressed in both glial cells and neurons under the control of the actin promoter was disappointing (Nagai et al. 2004). However, when we directed expression to only glial cells, the indicator's dynamic range of responses in cells *in situ* was comparable to what is observed in single cell experiments. The newer generation of CFP-YFP-based Ca^{2+} indicators using troponin-C instead of calmodulin, such as Cer-TN-L15 promise to be far superior to the YC cameleons. In our hands, YC 3.60 turned out to be a highly desirable indicator of physiological activity in tissues when targeted to glial cells (astrocytes) in mice.

In summary, we have utilized a genetically encoded Ca^{2+} indicator cameleon together with the astrocyte and Schwann cell-specific S100β promoter and targeted expression of YC 3.60 mainly in astrocytes in the CNS and Schwann cells in the PNS. As expected, YC 3.60 expression extended to all cells known to contain S100β protein. This obviates the need to load cells with Ca^{2+} indicators by patch clamping or microinjection. We show here that the expression level gives good signal-to-noise ratios in measurements of dynamic Ca^{2+} signals associated with physiological activity in individual cells as well as in microdomains of cells. Furthermore, sensory stimulation in anaesthetized mice evoked astrocytic Ca^{2+} signals in the somatosensory cortex. The experiments we present here suggest that these lines of transgenic mice may become highly desirable tools to investigate a number of outstanding questions in the field of neuron-glia signaling in detail. Current theories concerning glial modulation of single synapses and synapse ensembles ensheathed by the same astrocyte can now be potentially tested in *in situ* experimental paradigms.

Supplementary Material

Refer to Web version on PubMed Central for supplementary material.

Acknowledgments

We wish to thank Dr. Ramin Mollaaghababa for discussions and guidance in the early phases of plasmid construction. We wish to thank Drs. Josh Lawrence, Newton Woo, and Ludovic Tricore for help in setting up the Clampex software and integrating it with the Multiclamp. This work was supported by funds from the Intramural Research Program of the National Institutes of Child Health and Human Development, National Institutes of Health.

References

Araque A, Parpura V, Sanzgiri RP, Haydon PG. Glutamate-dependent astrocyte modulation of synaptic transmission between cultured hippocampal neurons. Eur J Neurosci. 1998; 10:2129–2142. [PubMed: 9753099]

Bushong EA, Martone ME, Ellisman MH. Examination of the relationship between astrocyte morphology and laminar boundaries in the molecular layer of adult dentate gyrus. J Comp Neurol. 2003; 462:241–251. [PubMed: 12794746]

Bushong EA, Martone ME, Jones YZ, Ellisman MH. Protoplasmic astrocytes in CA1 stratum radiatum occupy separate anatomical domains. J Neurosci. 2002; 22:183–192. [PubMed: 11756501]

Dani JW, Chernjavsky A, Smith SJ. Neuronal activity triggers calcium waves in hippocampal astrocyte networks. Neuron. 1992; 8:429–440. [PubMed: 1347996]

Diez-Garcia J, Matsushita S, Mutoh H, Nakai J, Ohkura M, Yokoyama J, Dimitrov D, Knopfel T. Activation of cerebellar parallel fibers monitored in transgenic mice expressing a fluorescent Ca2+ indicator protein. Eur J Neurosci. 2005; 22:627–635. [PubMed: 16101744]

Duffy S, MacVicar BA. Adrenergic calcium signaling in astrocyte networks within the hippocampal slice. J. Neurosci. 1995; 15:5535–5550. [PubMed: 7643199]

Fellin T, Pascual O, Gobbo S, Pozzan T, Haydon PG, Carmignoto G. Neuronal synchrony mediated by astrocytic glutamate through activation of extrasynaptic NMDA receptors. Neuron. 2004; 43:729–743. [PubMed: 15339653]

Fiacco TA, Agulhon C, Taves SR, Petravicz J, Casper KB, Dong X, Chen J, McCarthy KD. Selective stimulation of astrocyte calcium in situ does not affect neuronal excitatory synaptic activity. Neuron. 2007; 54:611–626. [PubMed: 17521573]

Fiacco TA, McCarthy KD. Intracellular astrocyte calcium waves in situ increase the frequency of spontaneous AMPA receptor currents in CA1 pyramidal neurons. J Neurosci. 2004; 24:722–732. [PubMed: 14736858]

Gordon S, Dickinson MH. Role of calcium in the regulation of mechanical power in insect flight. Proc Natl Acad Sci U S A. 2006; 103:4311–4315. [PubMed: 16537527]

Gravel M, Di Polo A, Valera PB, Braun PE. Four-kilobase sequence of the mouse CNP gene directs spatial and temporal expression of lacZ in transgenic mice. J Neurosci Res. 1998; 53:393–404. [PubMed: 9710259]

Gray NW, Weimer RM, Bureau I, Svoboda K. Rapid redistribution of synaptic PSD-95 in the neocortex in vivo. PLoS Biol. 2006; 4:e370. [PubMed: 17090216]

Grosche J, Matyash V, Moller T, Verkhratsky A, Reichenbach A, Kettenmann H. Microdomains for neuron-glia interaction: parallel fiber signaling to Bergmann glial cells. Nature Neursci. 1999; 2:139–143.

Hachem S, Aguirre A, Vives V, Marks A, Gallo V, Legraverend C. Spatial and temporal expression of S100B in cells of oligodendrocyte lineage. Glia. 2005; 51:81–97. [PubMed: 15782413]

Hasan MT, Friedrich RW, Euler T, Larkum ME, Giese G, Both M, Duebel J, Waters J, Bujard H, Griesbeck O, Tsien RY, Nagai T, Miyawaki A, Denk W. Functional fluorescent Ca2+ indicator proteins in transgenic mice under TET control. PLoS Biol. 2004; 2:e163. [PubMed: 15208716]

Heim N, Garaschuk O, Friedrich MW, Mank M, Milos RI, Kovalchuk Y, Konnerth A, Griesbeck O. Improved calcium imaging in transgenic mice expressing a troponin C-based biosensor. Nat Methods. 2007; 4:127–129. [PubMed: 17259991]

Heim N, Griesbeck O. Genetically encoded indicators of cellular calcium dynamics based on troponin C and green fluorescent protein. J Biol Chem. 2004; 279:14280–14286. [PubMed: 14742421]

Hirase H, Qian L, Bartho P, Buzsaki G. Calcium dynamics of cortical astrocytic networks in vivo. PLoS Biol. 2004; 2:E96. [PubMed: 15094801]

Hogan, B. Manipulating the mouse embryo: A lab manual. Cold Spring Harbor Press; 1994.

Holtmaat A, Wilbrecht L, Knott GW, Welker E, Svoboda K. Experience-dependent and cell-type-specific spine growth in the neocortex. Nature. 2006; 441:979–983. [PubMed: 16791195]

Holtzclaw LA, Pandhit S, Bare DJ, Mignery GA, Russell JT. Astrocytes in adult rat brain express type 2 inositol 1,4,5-trisphosphate receptors. Glia. 2002; 39:69–84. [PubMed: 12112377]

Imai Y, Ibata I, Ito D, Ohsawa K, Kohsaka S. A novel gene iba1 in the major histocompatibility complex class III region encoding an EF hand protein expressed in a monocytic lineage. Biochem Biophys Res Commun. 1996; 224:855–862. [PubMed: 8713135]

Ito D, Imai Y, Ohsawa K, Nakajima K, Fukuuchi Y, Kohsaka S. Microglia-specific localisation of a novel calcium binding protein, Iba1. Brain Res Mol Brain Res. 1998; 57:1–9. [PubMed: 9630473]

Jabs R, Pivneva T, Huttmann K, Wyczynski A, Nolte C, Kettenmann H, Steinhauser C. Synaptic transmission onto hippocampal glial cells with hGFAP promoter activity. J Cell Sci. 2005; 118:3791–3803. [PubMed: 16076898]

Kang J, Jiang L, Goldman SA, Nedergaard M. Astrocyte-mediated potentiation of inhibitory synaptic transmission. Nat Neurosci. 1998; 1:683–692. [PubMed: 10196584]

Kerr R, Lev-Ram V, Baird G, Vincent P, Tsien RY, Schafer WR. Optical imaging of calcium transients in neurons and pharyngeal muscle of C. elegans. Neuron. 2000; 26:583–594. [PubMed: 10896155]

Konnerth A, Orkand PM, Orkand RK. Optical recording of electrical activity from axons and glia of frog optic nerve: potentiometric dye responses and morphometrics. Glia. 1988; 1:225–232. [PubMed: 2852172]

Kriegler S, Chiu SY. Calcium signalling of glial cells along mammalian axons. J. Neurosci. 1993; 13:4229–4245. [PubMed: 7692011]

Kulik A, Haentzsch A, Luckermann M, Reichelt W, Ballanyi K. Neuron-glia signaling via a1 adrenoceptor-mediated Ca^{2+} release in Bergmann glial cells *in situ*. J. Neurosci. 1999; 19:8401–8408. [PubMed: 10493741]

Lyons SA, Morell P, McCarthy KD. Schwann cells exhibit P2Y purinergic receptors that regulate intracellular calcium and are up-regulated by cyclic AMP analogues. J Neurochem. 1994; 63:552–560. [PubMed: 8035179]

Mank M, Reiff DF, Heim N, Friedrich MW, Borst A, Griesbeck O. A FRET-based calcium biosensor with fast signal kinetics and high fluorescence change. Biophys J. 2006; 90:1790–1796. [PubMed: 16339891]

Matthias K, Kirchhoff F, Seifert G, Huttmann K, Matyash M, Kettenmann H, Steinhauser C. Segregated expression of AMPA-type glutamate receptors and glutamate transporters defines distinct astrocyte populations in the mouse hippocampus. J Neurosci. 2003; 23:1750–1758. [PubMed: 12629179]

Miyawaki A, Liopis J, Helm R, McCaffery JM, Adams JA, Ikurai M, Tsien RY. Fluorescent indicators for Ca^{2+} based on green fluorescent protiens and calmodulin. Nature. 1997; 388:882–887. [PubMed: 9278050]

Mostany R, Portera-Cailliau C. A craniotomy surgery procedure for chronic brain imaging. J Vis Exp. 2008

Nagai T, Yamada S, Tominaga T, Ichikawa M, Miyawaki A. Expanded dynamic range of fluorescent indicators for Ca(2+) by circularly permuted yellow fluorescent proteins. Proc Natl Acad Sci U S A. 2004; 101:10554–10559. [PubMed: 15247428]

Nett WJ, Oloff SH, McCarthy KD. Hippocampal Astrocytes In Situ Exhibit Calcium Oscillations That Occur Independent of Neuronal Activity. J. Neurophysiol. 2002; 87:528–537. [PubMed: 11784768]

Parpura V, Basarsky TA, Liu F, Jeftinija K, Jeftinija S, Haydon PG. Glutamate-mediated astrocyte-neuron signalling. Nature. 1994; 369:744–747. [PubMed: 7911978]

Pascual O, Casper KB, Kubera C, Zhang J, Revilla-Sanchez R, Sul JY, Takano H, Moss SJ, McCarthy K, Haydon PG. Astrocytic purinergic signaling coordinates synaptic networks. Science. 2005; 310:113–116. [PubMed: 16210541]

Perea G, Araque A. Properties of synaptically evoked astrocyte calsium signal reveal synaptic information processing by astrocytes. J. Neurosci. 2005; 25:2192–2203. [PubMed: 15745945]

Pologruto TA, Yasuda R, Svoboda K. Monitoring neural activity and [Ca2+] with genetically encoded Ca2+ indicators. J Neurosci. 2004; 24:9572–9579. [PubMed: 15509744]

Porter JT, McCarthy KD. GFAP-positive hippocampal astrocytes in situ respond to glutamatergic neuroligands with increases in $[Ca^{2+}]_i$. Glia. 1995; 13:101–112. [PubMed: 7544323]

Porter JT, McCarthy KD. Hippocampal astrocytes *in situ* respond to glutamate released from synaptic terminals. J. Neurosci. 1996; 16:5073–5082. [PubMed: 8756437]

Reiff DF, Ihring A, Guerrero G, Isacoff EY, Joesch M, Nakai J, Borst A. In vivo performance of genetically encoded indicators of neural activity in flies. J Neurosci. 2005; 25:4766–4778. [PubMed: 15888652]

Robitaille R. Modulation of synaptic efficacy and synaptic depression by glial cells at the frog neuromuscular junction. Neuron. 1998; 21:847–855. [PubMed: 9808470]

Rossner M, Yamada KM. What's in a picture? The temptation of image manipulation. J. Cell. Biol. 2004; 166:11–15. [PubMed: 15240566]

Schipke CG, Kettenmann H. Astrocyte responses to neuronal activity. Glia. 2004; 47:226–232. [PubMed: 15252811]

Shummers J, Yu H, Sur M. Tuned Responses of Astrocytes and Their Influence on Hemodynamic Signals in the Visual Cortex. Science. 2008; 320:1638–1643. [PubMed: 18566287]

Sprinkle TJ. 2',3'-cyclic nucleotide 3'-phosphodiesterase, an oligodendrocyte-Schwann cell and myelin-associated enzyme of the nervous system. Crit Rev Neurobiol. 1989; 4:235–301. [PubMed: 2537684]

Stellwagen D, Malenka RC. Synaptic scaling mediated by glial TNF-alpha. Nature. 2006; 440:1054–1059. [PubMed: 16547515]

Sul JY, Orosz G, Givens RS, Haydon PG. Astrocytic Connectivity in the Hippocampus. Neuron Glia Biol. 2004; 1:3–11. [PubMed: 16575432]

Suzuki H, Kerr R, Bianchi L, Frokjaer-Jensen C, Slone D, Xue J, Gerstbrein B, Driscoll M, Schafer WR. In vivo imaging of C. elegans mechanosensory neurons demonstrates a specific role for the MEC-4 channel in the process of gentle touch sensation. Neuron. 2003; 39:1005–1017. [PubMed: 12971899]

Takano T, Tian GF, Peng W, Lou N, Libionka W, Han X, Nedergaard M. Astrocyte-mediated control of cerebral blood flow. Nat Neurosci. 2005; 9:260–267. [PubMed: 16388306]

Vives V, Alonso G, Solal AC, Joubert D, Legraverend C. Visualization of S100B-positive neurons and glia in the central nervous system of EGFP transgenic mice. J Comp Neurol. 2003; 457:404–419. [PubMed: 12561079]

Wallraff A, Odermatt B, Willecke K, Steinhauser C. Distinct types of astroglial cells in the hippocampus differ in gap junction coupling. Glia. 2004; 48:36–43. [PubMed: 15326613]

Wang X, Lou N, Xu Q, Tian GF, Peng WG, Han X, Kang J, Takano T, Nedergaard M. Astrocytic Ca2+ signaling evoked by sensory stimulation in vivo. Nat Neurosci. 2006; 9:816–823. [PubMed: 16699507]

Zhou M, Kimelberg HK. Freshly isolated hippocampal CA1 astrocytes comprise two populations differing in glutamate transporter and AMPA receptor expression. J Neurosci. 2001; 21:7901–7908. [PubMed: 11588163]

Zuo Y, Lubischer JL, Kang H, Tian L, Mikesh M, Marks A, Scofield VL, Maika S, Newman C, Krieg P, Thompson WJ. Fluorescent proteins expressed in mouse transgenic lines mark subsets of glia, neurons, macrophages, and dendritic cells for vital examination. J Neurosci. 2004; 24:10999–11009. [PubMed: 15590915]

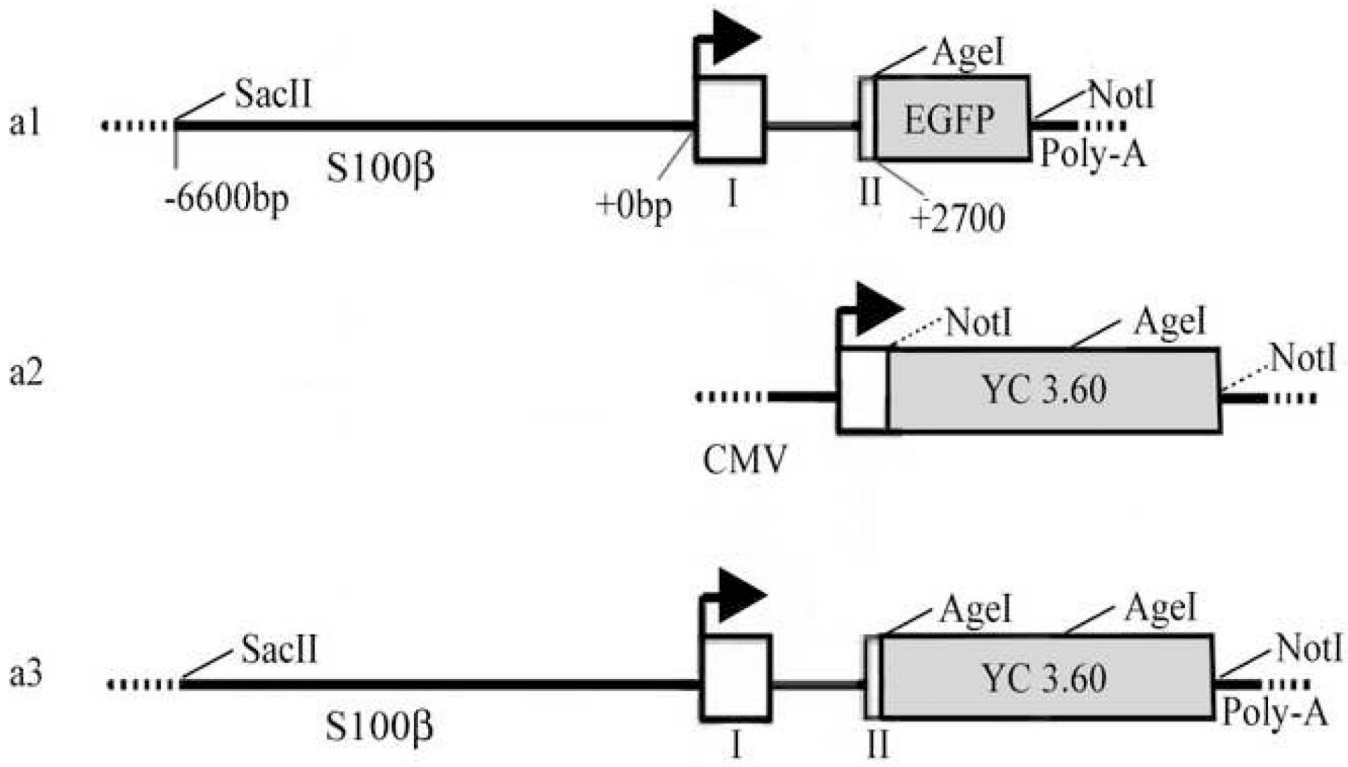

Figure 1.

Design of pS100β-YC 3.60 from previously derived vectors. *A*, S100β-EGFP(a1), pCMV-YC 3.60(a2), and the S100β-YC 3.60(a3) construct. Restriction enzyme sites are labeled. The *NotI* site 5' to YC 3.60 in a2 was mutated by PCR to an *AgeI* site for compatibility with the 3' end of the S100β promoter.

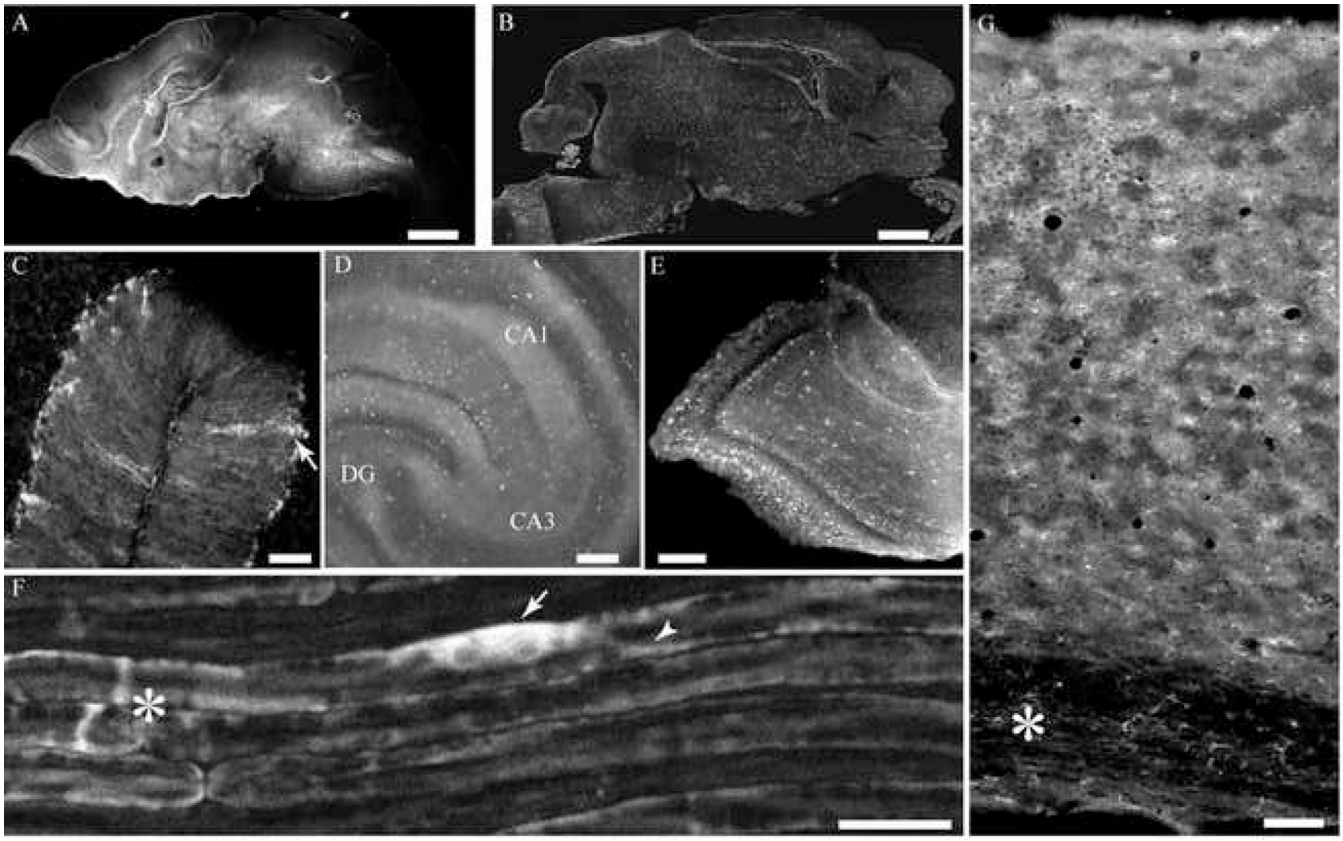

Figure 2.

Expression of YC 3.60 in brain and peripheral nerves in transgenic F1 generation mice. Brains from 2 day old pups were fixed and sectioned in a cryostat as described in Methods and imaged without staining (A) or developed for immunohistochemistry using anti-GFP antibodies. *A*, A sagittal section from a S100β-YC-C mouse brain shows native YC 3.60 fluorescence imaged without staining (scale bar = 150 μm). *B*, Another section prepared as in A was developed for immunohistochemistry using anti-GFP antibodies and Rhodamine Red-X conjugated secondary antibodies (scale bar = 150 μm). Immunohistochemistry amplifies the signal compared with native YC 3.60 fluorescence. The transgenic mouse brain sections shows a large number of brightly stained cells that appear to be astrocytes, *C*, cerebellum; *D*; hippocampus, *E*; olfactory bulb (scale bars in C to E = 50 μm). *F*, Image of sciatic nerve from a S100β-YC-P mouse imaged intact through the perineureum shows myelinated axons brightly fluorescent with YC 3.60. The nerve was excited at 805 nm and YFP and CFP emissions were collected. Note intense YC 3.60 fluorescence in the Schwann cell soma (arrow), and Cajal bands (arrow head). The asterisk denotes a node of Ranvier (scale bar = 20 μm). *G*, Image of a section through the cortex from a S100β-YC-C mouse brain. Pial surface is at the top, and corpus callosum at the bottom (asterisk).

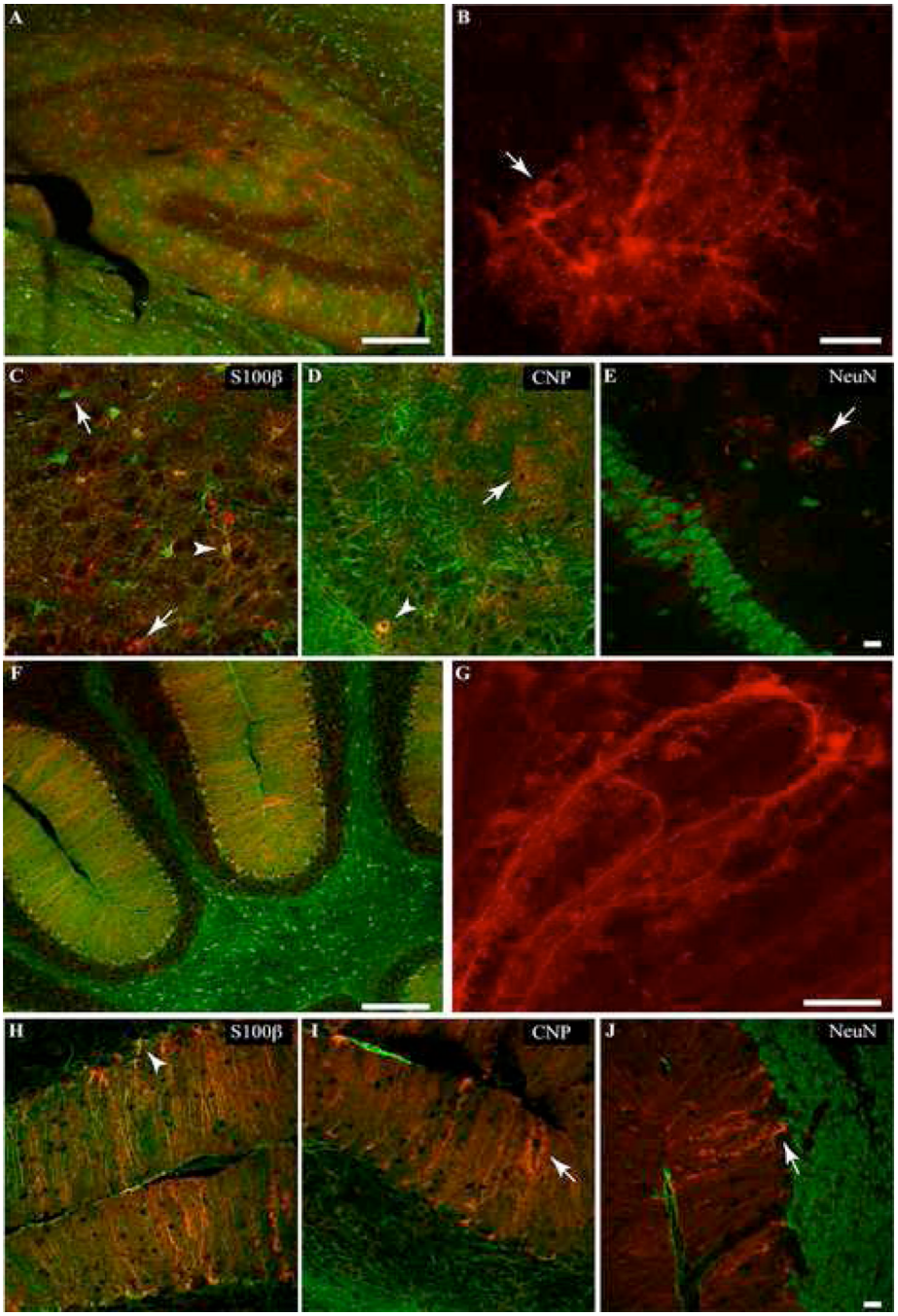

Figure 3.

Immunohistochemical localization of YC 3.60 (red) and cell specific markers (green) in the adult S100β-YC-C hippocampus, and cerebellum. Arrowheads mark colocalization of anti-GFP staining with the cell specific marker, and arrows mark cells with non-overlapping stains. *A*, Widefield image of hippocampus dual stained with anti-GFP and anti-S100β antibodies. YC 3.60 staining overlaps with the majority of S100β positive cells (Scale bar = 200 μm). *B*, A maximum intensity projection of confocal slices of a single YC 3.60 and S100β positive astrocyte in the hippocampus (the green S100β stain has been turned off. Scale bar = 10 μm). *C–E*, Individual .8μm confocal slices from the hippocampus. YC 3.60 staining colocalizes (arrow heads) with S100β (astrocyte marker), and CNP (marker for

oligodendrocyte lineage cells), but not NeuN, a neuronal marker. Note in *C* and *D* that cells stained for either S100β, CNP or YC 3.60 alone can be found (arrows). YC 3.60 was not found in myelin or in NeuN-positive neuronal cell bodies (Scale bar = 20 μm). *F*, Low magnification view of the cerebellum shows YC 3.60 and S100β colocalization in Bergmann glial cells. A number of S100β-containing astrocytes, however, show very low levels of YC 3.60 content. *G*, Maximum intensity projection of confocal slices from a S100β-positive Bergmann glial cell expressing YC 3.60 (S100β staining has been turned off. Scale bar = 20 μm). *H–J*, Individual 0.8μm confocal slices from a cerebellar section. Staining for YC 3.60 is found primarily in Bergmann glial cells (arrow head in H), very rarely in CNP-positive cells of the oligodendrocyte lineage (I), and not in NeuN-positive neurons (J, Scale bar = 20 μm).

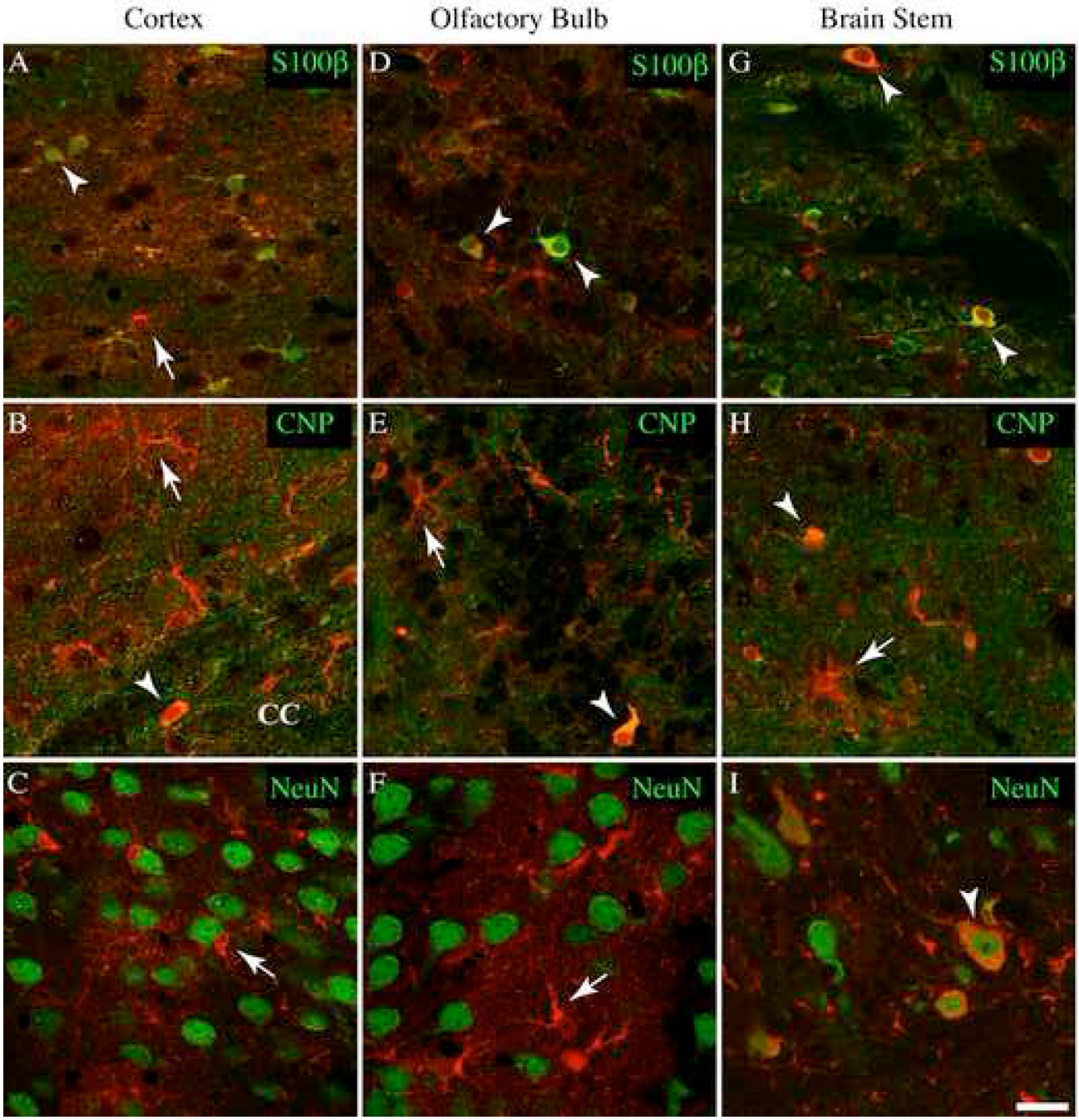

Figure 4.

YC 3.60 expression within the cortex, olfactory bulb, and brain stem. Immunohistochemistry of YC 3.60 (red) and cell markers (green); S100β (astrocytes), CNP (oligodendrocyte lineage cells), and NeuN (neurons) in a section from a S100β-YC-C mouse. All images are individual confocal (0.8μm) optical slices. Arrowheads mark overlapping stains, while arrows indicate non-colocalized stains. *A–C*, In the cortex, YC 3.60 is predominately found in S100β-positive astrocytes (arrowheads). Cells stained for either S100β or GFP alone are indicated. A few YC 3.60-positive cells in the corpus callosum (CC), and in Layer IV are CNP-positive. These cells are most likely oligodendrocytes (B). NeuN staining did not reveal any neurons expressing YC 3.60 (C). *D–*

F, Olfactory cells expressing YC 3.60 are either S100β-positive astrocytes, or CNP-positive oligodendrocytes. NeuN staining did not colocalize with YC 3.60 positive cells. *G–I*, Staining in the brain stem revealed a pattern of S100β and CNP cell expression similar to that in the olfactory bulb. *I*, YC 3.60 was expressed in a number of the large motor neurons of the brain stem (Scale bar = 20 μm).

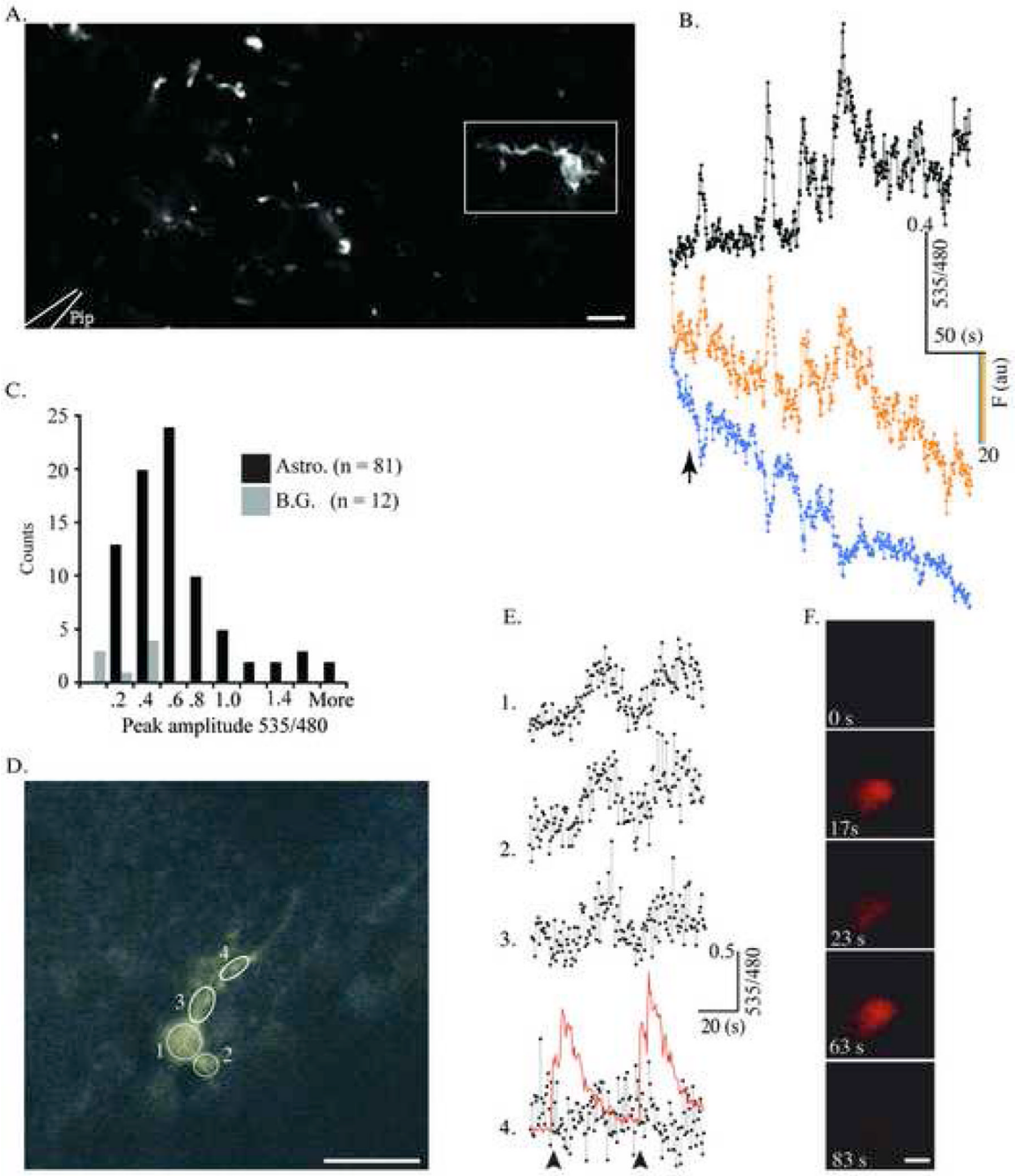

Figure 5.

YC 3.60-expressing glia respond to glutamate *in situ*. *A.* YC 3.60-containing astrocytes in a cortical slice (S100β-YC-C mouse) were imaged in a Zeiss Upright two-Photon microscope using non-descanned detectors. A picospritzer ejected 100nL of 500μM glutamate from a 1 MΩ resistance pipette tip (represented by white outlines at bottom left. Scale bar = 50 μm). In this focal plane, only one cell is visible and the rest of the fluorescent profiles are parts of cells. Images (512×256 pixels) were acquired at 2Hz (1.6μs pixel dwell time). *B,* The change in 535/480 during glutamate ejection (arrow) for the cell within the rectangle in A (black trace, top). The traces in color (cyan and yellow) are single wavelength traces at 480 and 535 nm respectively. *C,* Frequency histogram of compiled data from all the experiments

(81 cells, 9 slices) shows YFP/CFP ratio change from baseline levels to peak amplitude upon glutamate addition (R/R_0). B.G. denotes background. *D*– *F*, Cerebellar Bergmann glia were imaged and treated identically to the cortical astrocytes in *A*. Images (256×256 Pixels) were acquired at 2Hz (1.92 μs pixel dwell time). Circles delineate ROIs drawn over the cell where measurements were made (Scale bar = 20 μm). In this experiment, glutamate within the microinjection pipette was spiked with Quantum Dot 655 nanocrystals to allow direct visualization of the glutamate injection during imaging. *E*, YC 3.60 reports Ca^{2+} activity in ROIs 1–4 in *D* during two sequential glutamate injections. The arrow represents the 1st microinjection of 300μM glutamate, and the red trace represents the QD 655 fluorescence following injection in the ROI 4 trace. *F*. Time-lapse stills of the QD 655/Glutamate microinjection with time points labeled. The diameter of the QD cloud is roughly twice the diameter of the Bergmann glial cell body (Scale bar = 20 μm).

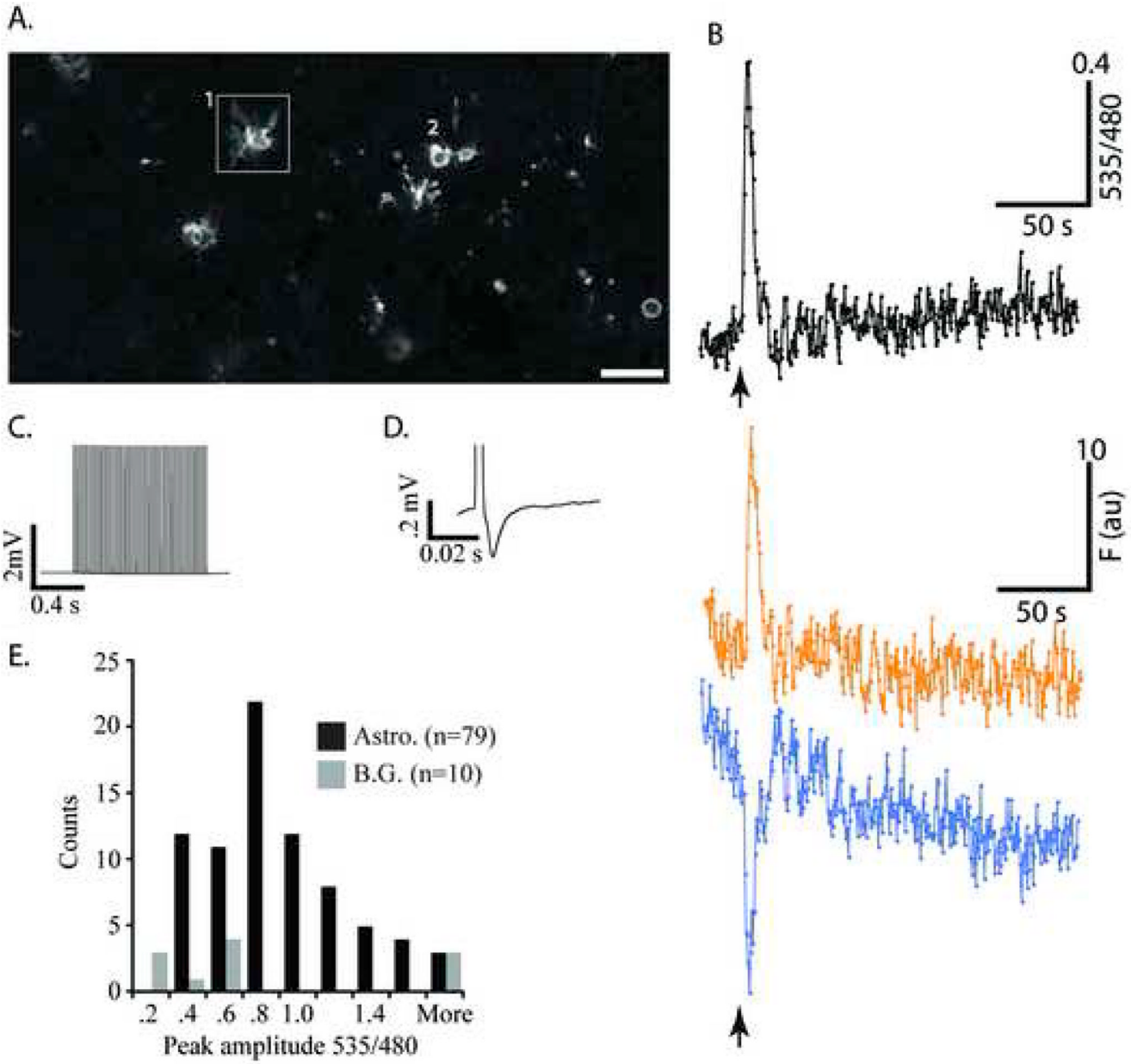

Figure 6.

Ca^{2+} waves in astrocytes reported by YC 3.60 during electrical stimulation of Schaffer collateral pathway in a hippocampal slice. *A*, Astrocytes in the *stratum radiatum* of the S100β-YC-C mouse, approximately 200μm away from the extracellular stimulus electrode (Scale bar = 100 μm). Images (512×256 pixels) were acquired at 2 Hz (1.6 μs pixel dwell time). *B*, Ratio fluorescence (535/480 nm) trace from the astrocyte within the box in *A*. Arrow marks when a 1 second, 50Hz, 100 μA electrical pulse train was delivered to Schaffer collaterals (black trace, top). The traces in color at the bottom (cyan and yellow) represent single wavelength data at 535 nm and 480 nm respectively. Note that this astrocyte responded with an instantaneous Ca^{2+} response followed by low level oscillations. *C*, A trace of the 50Hz stimulus train and a single field potential recorded from the CA1 pyramidal dendrite layer *D. E*, Frequency histogram of the peak amplitude (R/R_0) responses in astrocytes and background (B.G.) areas in the slice evoked by the stimulus protocol. Note

that most astrocytes show a 20 to 70% increase in YFP/CFP ratio, and the background regions a 10 to 50% increase.

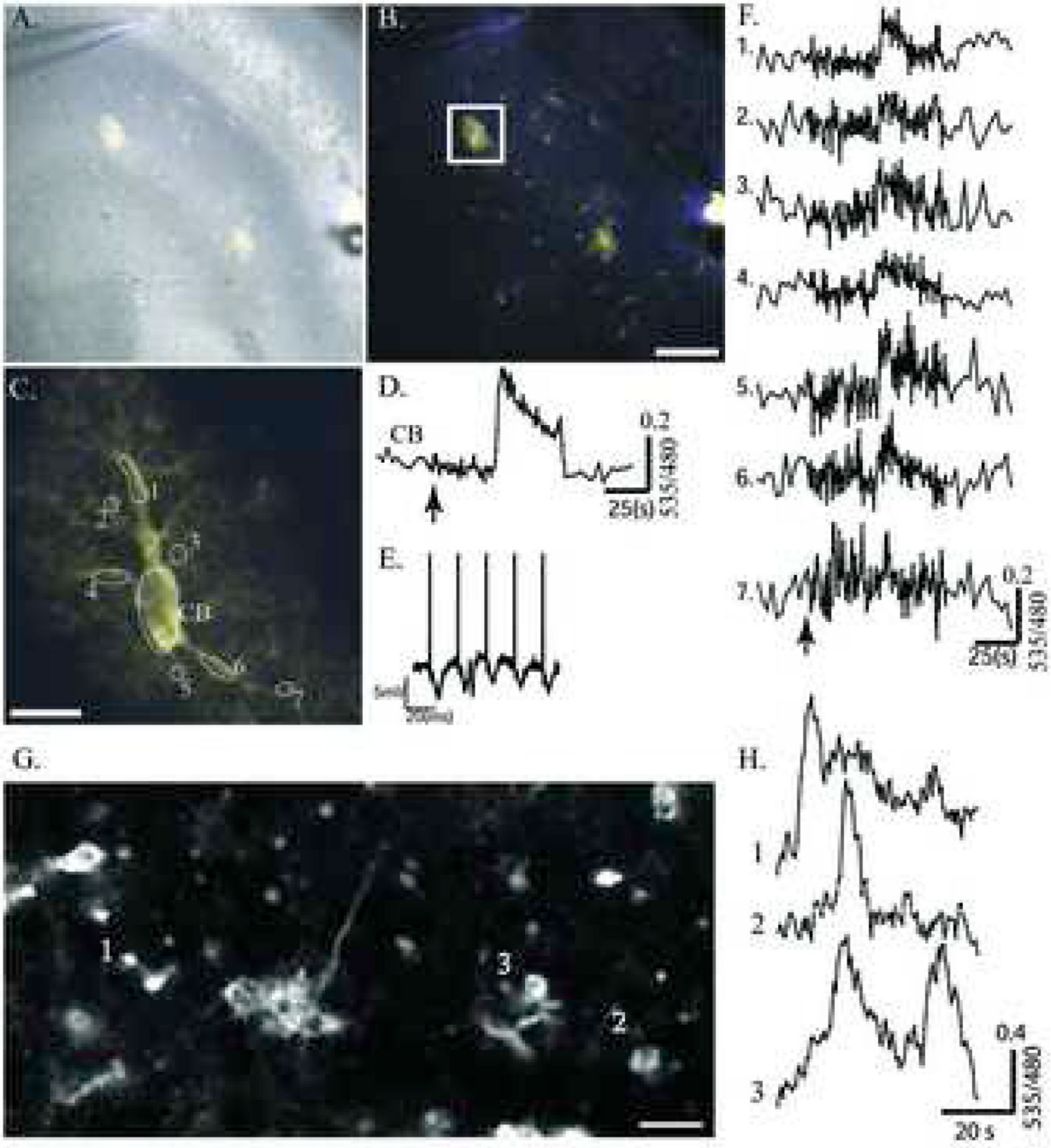

Figure 7.

Ca^{2+} activity visualized in single astrocyte processes during hippocampus mossy fiber stimulation in the S100β-YC-B mouse. *A*, Overlay of bright field and transgenic YC 3.60 fluorescence in area CA3. The recording electrode can be seen in the upper left, and the stimulus electrode in the lower right of the pyramidal cell layer. *B*, Same as *A* without the bright field overlay (Scale bar = 100 μm). Images (512×512 pixels) were acquired at a rate of 1Hz (1.6 μs pixel dwell time). *C*, The cell bounded by the box in *B* was monitored at high magnification during mossy fiber stimulation (1s, at 50Hz, 100μA). *D*, YFP/CFP ratio trace from the cell body (CB). *E*, Field potentials recorded in response to the first 5 stimuli in the stimulus train. *F*, Traces 1 to 7 show YFP/CFP ratios measured in the ROIs 1 to 7

(numbered in C). Stimulus occurs at the arrow. *G*, A two-photon image from *Stratum Oriens* near the CA1 pyramidal cell layer shows spontaneous Ca^{2+} activity (Scale bar = 10 μm). Images (512×256 pixels) were acquired at 2Hz (1.6μs pixel dwell time). *H*, Ratio fluorescence (535/480 nm) traces obtained from three individual cells are plotted to show asynchronous spontaneous activity.

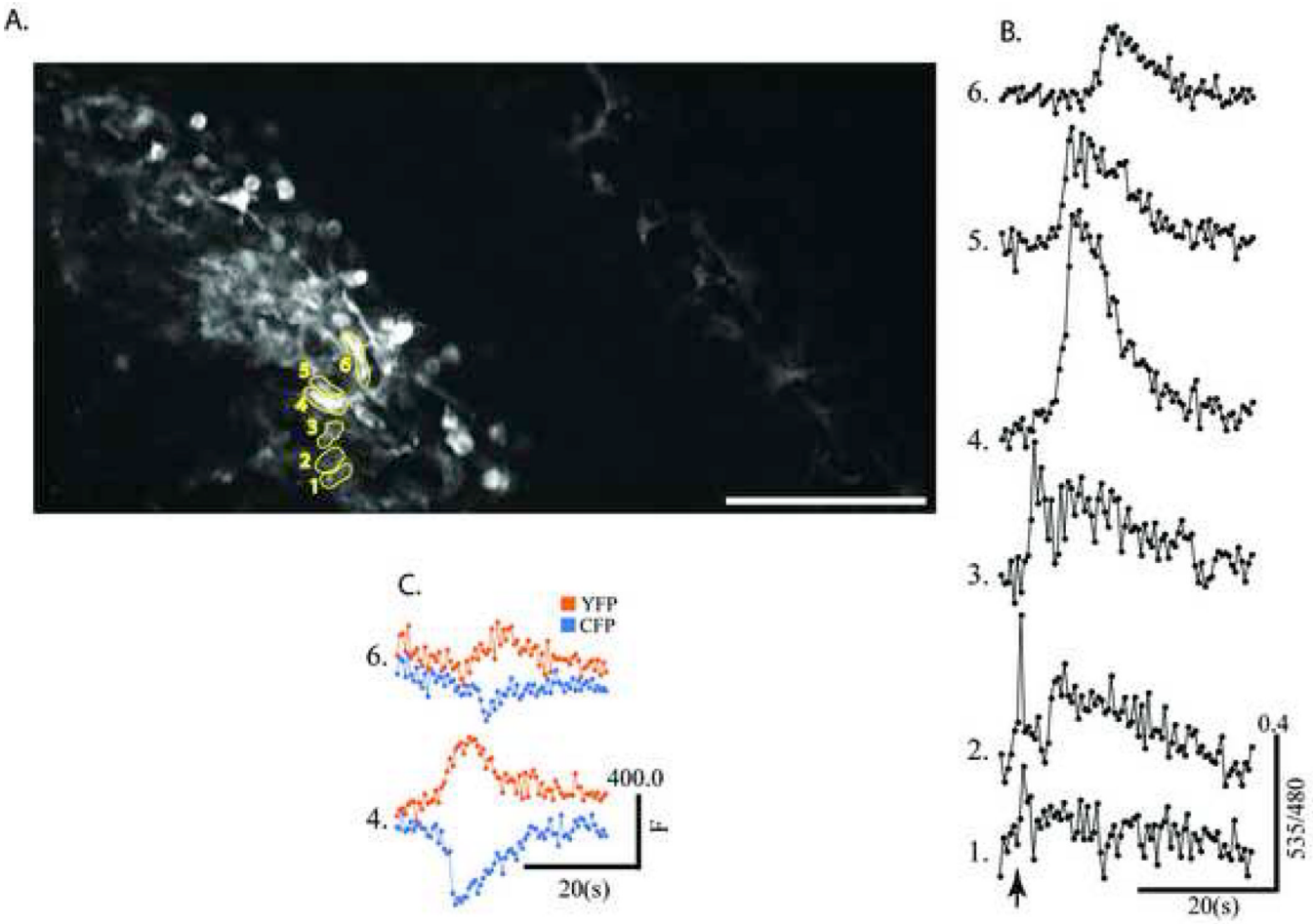

Figure 8.

In vivo recordings of astrocytic Ca^{2+} signals. YC 3.60-containing astrocytes in layer 2/3 cortex were imaged by 2-photon microscopy through a cranial window in an anaesthetized live mouse from the S100β-YC-C line. Only one or two fields can be imaged through the 3 mm window, but imaging extended as far as 250 μm deep within the cortex (see also Supplementary Figures 5 and 6). Images (512×256 pixels) were acquired at a rate of 2Hz, (1.6 μs pixel dwell time). While imaging, the forepaw of the mouse was stimulated using small (27 gauge) needle electrodes for 3 s (50 Hz, 1.5 mA, 100 μs, pulses, arrow in *B*). *A*, Glial cells (putative astrocytes) containing YC 3.60 fluorescence in the field (Scale = 100 μm). Note also labeled cells away from focal plane on the right side of the field. *B*, Traces showing 535/475 ratio plotted against time. Traces represent data derived from the cells outlined and numbered in panel *A*. Note the astrocytic Ca^{2+} response begins at the bottom of the field and spreads as a wave upwards. *C*, Single wavelength fluorescence intensity data (CFP, Blue, and YFP, Yellow) derived from cells numbered 4 and 6 in *A*.

Table 1

Pattern of YC 3.60 transgene expression

Region Line	Cortex	Cere- bellum	Hippocampus	Olfactory Bulb	Corpus Callosum	Brain Stem	Sciatic nerve
2547 S100β-YC-C	++++ intense	++++ intense	+++ bright	++++ intense	++ visible	++ visible	+ dim
2604 S100β-YC-B	++++ intense	++++ intense	++++ intense	++++ intense	++ visible	++ visible	+ dim
2622 Not used	+++ bright	++ visible	++ visible	+++ bright	++ visible	++ visible	+ dim
2562 S100β-YC-P	+ dim	+ dim	+ dim	+ dim	+ dim	+ dim	++++ intense

Table 2

Percentage of GFP containing cells with cell-specific marker

Transgenic line 2547						
Region Cell Marker	**Cortex**	**Cere-bellum**	**Hippo-campus**	**Olfactory Bulb**	**Corpus Callosum**	**Brain stem**
S100β	67.4±4.6	61.9±14.1	99.1±1.8	65.6±1.8	ND	72.3±13.2
CNP	26.7 ±8.2	16.4±2.9	ND	38.4±6.9	ND	26.5±2.5
iba	38.7±19.7	26.3±9.0	33.3±16.1	16.6±2.7	28.4±13.6	17.7±1.1
Neu-N	0	0	0	0	0	29.7±3.0
Transgenic line **2604**						
S100β	65.8±19.7	73.3±9.9	79.0±14.2	67.4±17.6	74.8±18.8	72.7±10.3
NG-2	0	0	0	0	0	0
iba	45.2±9.8	25.0±16.3	9.9±16.3	38.7±13.1	15.5±14.8	26.7±16.1
Neu-N	0	0	0	0	0	47.2±15.8

Table 3

Percentage of S100β-containing astrocytes expressing GFP

Region Cell Marker	Cortex	Cere- bellum	Hippo- campus	Olfactory Bulb	Corpus Callosum	Brain stem
S100β-YC-C	60.0±2.3	78.5±3.9	51.8±4.2	81.3±2.5	ND	64.7±10.5
S100β-YC-B	23.9±10.4	62.3±19.0	22.7±6.1	16.5±6.6	11.7±4.4	44.9±9.8